RESEARCH ARTICLE

*Geoarchaeology* An International Journal  **WILEY**

# Geochemical analysis of the truncated Viking Age trading settlement of Heimdalsjordet, Norway

Rebecca J. S. Cannell[1,3] 🔟 | Jan Bill[2] | Paul Cheetham[1] | Kate Welham[1]

[1]Department of Archaeology, Anthropology and Forensic Sciences, Bournemouth University, Poole, UK

[2]Department of Archaeology, Museum of Cultural History, University of Oslo, Oslo, Norway

[3]Department of Archaeology, Conservation and History, University of Oslo, Oslo, Norway

**Correspondence**
Rebecca J. S. Cannell, Department of Archaeology, Conservation and History, University of Oslo, Oslo, Norway.
Email: rebecca.cannell@iakh.uio.no

**Abstract**

Single and multielement archaeological geochemistry has been applied to research and rescue projects for many decades to enhance our understanding of the past use of space. Often applied on one contextual plane, this ignores the complex palimpsest resulting from past occupation and soil processes. Furthermore, many important sites are now heavily truncated by plowing, leaving little more than negative features below the homogenized topsoil. These challenges require new approaches to archaeological geochemistry to gather information before these sites are lost to modern land use. The research presented here applied coring as a sampling method on a truncated site, the sample locations guided by high-resolution ground-penetrating radar data and excavation, before using portable X-ray fluorescence directly on the core samples to understand the phase by phase composition of the deposits and thus past human occupation. The results suggest that even in truncated and secondary contexts, such as the case study of the Viking Age trade settlement of Heimdalsjordet, Norway, archaeological geochemistry can give insight into the chronological and spatial development of the site, and is especially relevant for detecting nonferrous metalworking activity.

**KEYWORDS**

coring, geochemistry, geophysics, pXRF, Viking Age

## 1 | INTRODUCTION

A means of understanding past settlements and the people within them is to understand how space was organized, utilized, and experienced over time. The site in focus here, Heimdalsjordet, is one of only two coastal trading sites from the Viking Period known in Norway, the other being the nearby site of Kaupang (Skre, 2007). Understanding the cultural organization of the site and the range of activities present as the site developed, that is the use of space, would provide a foundation for comparison between sites in terms of its role in social and economic networks. While the theoretical perspectives on the use of space are not the focus here; they are an integral part of this project. The use of space, as a social and physical construct, is fundamental to our understanding of the world around us. We label space in a culturally specific way, but it is also something that is created and morphed as it simultaneously mediates social interactions (Kühtreiber, 2014; Lefebvre, 1991). Space can be viewed as a manifestation of socially constructed and accepted behaviors that are environmentally responsive (Løvschal & Holst, 2014)). How people engage and live within spatial divisions can be seen as the incremental accumulation of behavioral responses to cultural and environmental factors. Over time, certain behaviors and responses become more prominent as they, consciously or unconsciously, are seen as more acceptable responses; what Løvschal and Holst (2014)

term a "spatial repertoire." Temporarily and change is added by shared references and retrospect within the context, which can be implemented, modified, or ignored by a person or group. This creates a dynamic between past and present, the individual and society. Therefore, how space is created and used is a gateway into the cultural past and a means of interpreting sites on many scales.

The site was heavily truncated by plowing, and predominantly consisted of negative features—that is archaeological features surviving as a backfilled cuts into the subsoil—such as ditches that divided the land into plots and parcels. The ditches at Heimdalsjordet predominantly divided the area into parcels; that is small ditched enclosures on the scale of small house sizes, and these parcels are within the larger plots. Some few of these ditches are more linear and/or interconnected, and can be associated with plot boundaries. In many cases, plots may have contained more than one small rectangular parcel, and may also have been additionally defined by, for example, fencing. In contemporary and broadly comparable sites such as Dublin, each plot contained one or two buildings, and perhaps some animals penning, but without space for farming (Wallace, 2016). To understand the use of space at Heimdalsjordet, new sampling approaches had to be developed to meet the challenges of the truncated archaeology.

This paper examines the intersection between the application of archaeological geochemistry, the nature of archaeological deposits in excavation and prospection contexts, the sampling methods applied in both methodologies, and their interpretations, as applied to the site of Heimdalsjordet.

## 1.1 | Sampling methods in geochemistry

Several reviews of archaeological geochemistry have been published, considering both the single element methods (e.g., Bethell & Máte, 1989; Holliday & Gartner, 2007) and multielement approaches (e.g., Oonk, Slomp, & Huisman, 2009; Walkington, 2010; Wilson, Davidson, & Cresser, 2008), as well as key papers that have forwarded knowledge of the relationship between relative elemental enhancement and depletion in archaeological contexts and how this can be measured and related to past human activity (e.g., Entwistle & Abrahams, 1997; Entwistle, Dodgshon, & Abrahams, 2000; Middleton, 2004; Milek & Roberts, 2013). The method has expanded in tandem with technological availability. Since the late 1980s, inductively coupled plasma mass spectrometry (ICP-MS)/optical emission spectrometry (OES)/atomic emission spectrometry (AES) have been the most commonly used techniques, exemplified by Bethell and Smith's (1989) paper and subsequent research (e.g., Entwistle, Abrahams, & Dodgshon, 1998; Luzzadder-Beach, Beach, Terry, & Doctor, 2011; Middleton, 2004; Sylvester, Mann, Rate, & Wilson, 2017; Wilson, Davidson, & Cresser, 2009). In recent years, the use of X-ray fluorescence (XRF) in portable or lab-based form, has become increasingly common (Booth et al., 2017; Cook, Clarke, & Fulford, 2005; Cook et al., 2010; Entwistle, Mccaffrey, & Abrahams, 2009; Gauss, Bátora, Nowaczinski, Rassmann, &

Schukraft, 2013; Hayes, 2013; Mikołajczyk & Schofield, 2017). Instrument selection involves additional decisions and restraints which ultimately dictate the data that can be collected, and this has been debated in relation to portable XRF (pXRF; Frahm, 2013; Hunt & Speakman, 2015; Speakman & Shackley, 2013). The concern is that the utilization of internal calibration and "point and shoot" instruments and methodologies creates inaccurate and imprecise data that, as uncalibrated to any external standard, is incomparable.

In archaeological geochemistry sampling, there is a strong tendency for methods to fall into one of two categories: sampling specific features only (Cook et al., 2010; Cook, Kovacevich, Beach, & Bishop, 2005; Couture, Bhiry, Monette, & Woollett, 2016; Luzzadder-Beach et al., 2011; Wilson, Davidson, & Cresser, 2007; Wilson et al., 2009) or areal sampling using a horizontal grid or transects within an archaeologically defined area (Jones et al., 2010; Middleton, 2004; Middleton et al., 2010; Oonk, Slomp, Huisman, & Vriend, 2009; Vyncke, Waelkens, Degryse, & Vassilieva, 2011). The first approach lays weight on function and activity. It ignores the significance of motion, reference and relationships in human-created spaces, focusing solely on the *what*. The second achieves more by way of spatial patterning and social/cultural relations, but often occurs on a single horizontal plane. Time, in effect, ceases to matter, and it assumes all is chronologically simultaneous, and so comparable, culturally and pedologically. In addition, the analytical space is not defined by the past population and society, but by the archaeologist. There are studies published which include down-section sampling, for single or multiple elements, however, these are often limited to one or two sections and then time becomes the only thing that matters (Crowther, 1997; Ottaway & Matthews, 1988; Salisbury, 2013).

When sampling occurs on a horizontal plane, a floor is often the target (if preserved), or a subsoil layer within an excavation, or some point in the topsoil for prospection. On a multiperiod site, when sampling one stratigraphic layer late in the excavation, the method becomes reliant on soil processes having paradoxically both leached and retained elemental enhancements from now removed phases and gathering them in one horizon. This can have some success, but it is not working with respect to the mechanisms within the soil the method relies upon. The present study attempted an alternative approach using coring as a sampling method to try and capture time and space within the secondary deposits, measured using pXRF directly on the cores.

Secondary contexts are defined as backfills in archaeological features which consist of a heterogeneous mix of locally derived residual material from the last phases of occupation and earlier activities. The sediments do not directly represent a sole activity or a deliberate assemblage. These compare to primary contexts, whose composition represents a deliberate act, and where the spatial distribution of enhancements in the sediment reflects the activity or process that purposively created them (Carver, 1995; Schiffer, 1976, p. 105). From a geochemical perspective, it is the preservation of spatial patterning from intentional and unintentional acts that defines whether they can be considered primary or not. The formation of archaeological deposits in negative features such as ditches can be a combination of factors, which can limit their potential interpretations.

## 1.2 | Heimdalsjordet

The site of Heimdalsjordet, located in Vestfold County, Norway (Figure 1), was investigated in 2012–2013 as part of the Gokstad Revitalised Project (GOREV). Heimdalsjordet was occupied in the early to mid-Viking Age (800–1050 A.D.), with the main phases of activity in the mid-Viking Age. The site is primarily composed of ditches arranged along a thoroughfare, comprising parcels of land and the ring ditches from plowed out burial mounds. The thoroughfare is an E-W orientated feature demarcated by the parcel ditches, fading to the east as the ground rises from around parcel 6 and on toward parcels 9–14 (see below) (Figure 2). Associated with parcels 9–14 and spreading east, was an occupation layer that followed the terrain a short distance toward the former stream course, which is now under modern landscaping (Figure 3). The areas investigated by excavation were selected from previous evaluation trenching and ground penetrating radar (GPR) data.

The parcel ditches varied in width and depth, most being rectangular or subrectangular, the largest measuring 14.5 m × 6.7 m, while smaller parcels measure, for example, 10 m × 5.5 m. Several are cut by later ditches, suggesting recutting over several phases of occupation on the site.

On comparable sites such as Ribe, Denmark, ditches defined boundaries, although the plots at Ribe were perhaps also separated by fencing (Feveile, 2008). At Heimdalsjordet, the ditches appear connected to activities within the parcels, rather than purely defining the plots themselves (Bill & Rødsrud, 2017). While many are too deep to be wall ditches, they could define building parcels within a larger land plot defined by fencing, the traces of which have not survived. Together with other forms of boundary, parceled land, and ditches form political, economic, and social boundaries for the occupants throughout the settlement lifespan.

Finds are predominantly dated to the Viking Age (800–1050 A.D.), including beads, metal fittings, ingots, and metalworking scrap and waste, Arabic dirhams, whetstones, weights and amber fragments. Based upon radiocarbon dating, the most likely date range for the early phase of the site is the very late 700s to early 800s, and the later phases date from the mid-8th to the mid-10th centuries. It appears the settlement fell out of use in the latter half of the 10th century (Bill & Rødsrud, 2017).

## 1.3 | The environmental setting

Postglacial eustatic rises caused the inundation of southern Norway by the sea, forming a marine-sourced depositional landscape far inland. Later isostatic rebound caused relative falls in sea levels, which have slowed to the current rate of 2–3 mm/year, however, in the Viking Age the rate is estimated to be ca. 3.5 mm/year (Sørensen,
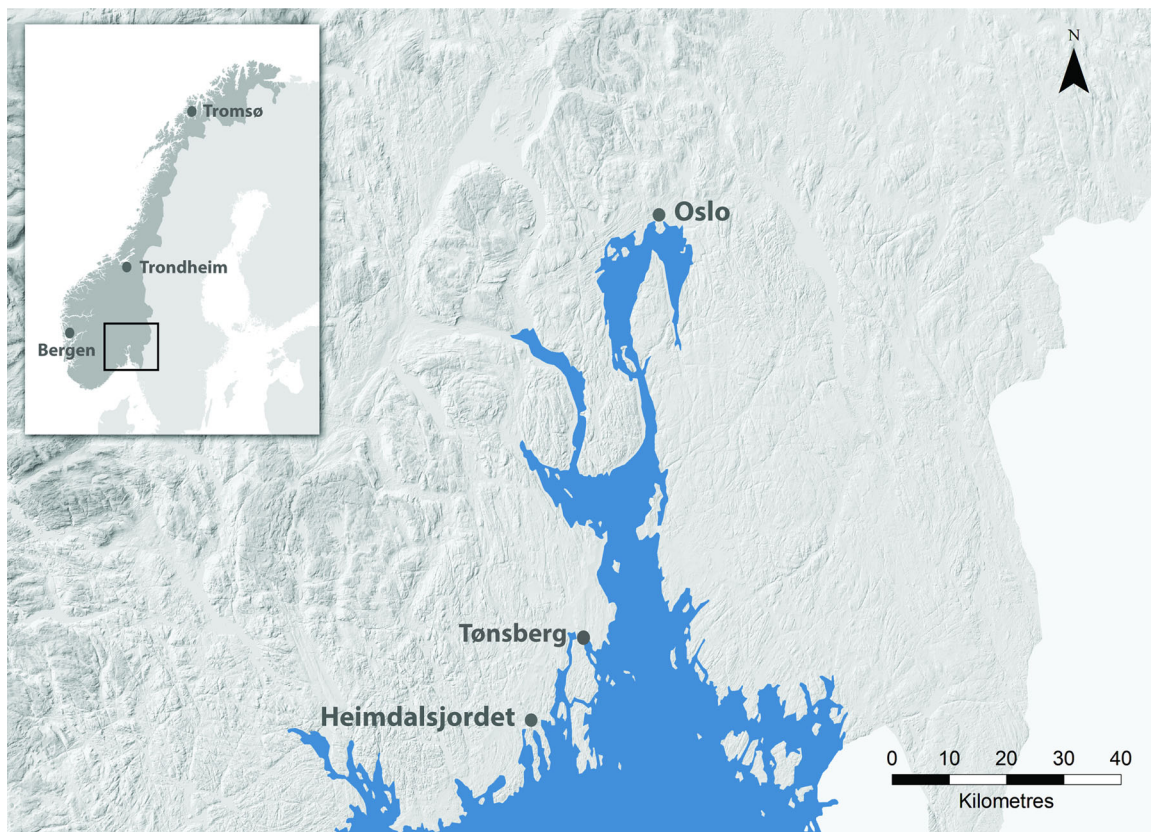


**FIGURE 1** Location map of the case study. Map Source: Norwegian Mapping Authority, Geovekst, and Municipalities 2020 [Color figure can be viewed at wileyonlinelibrary.com]
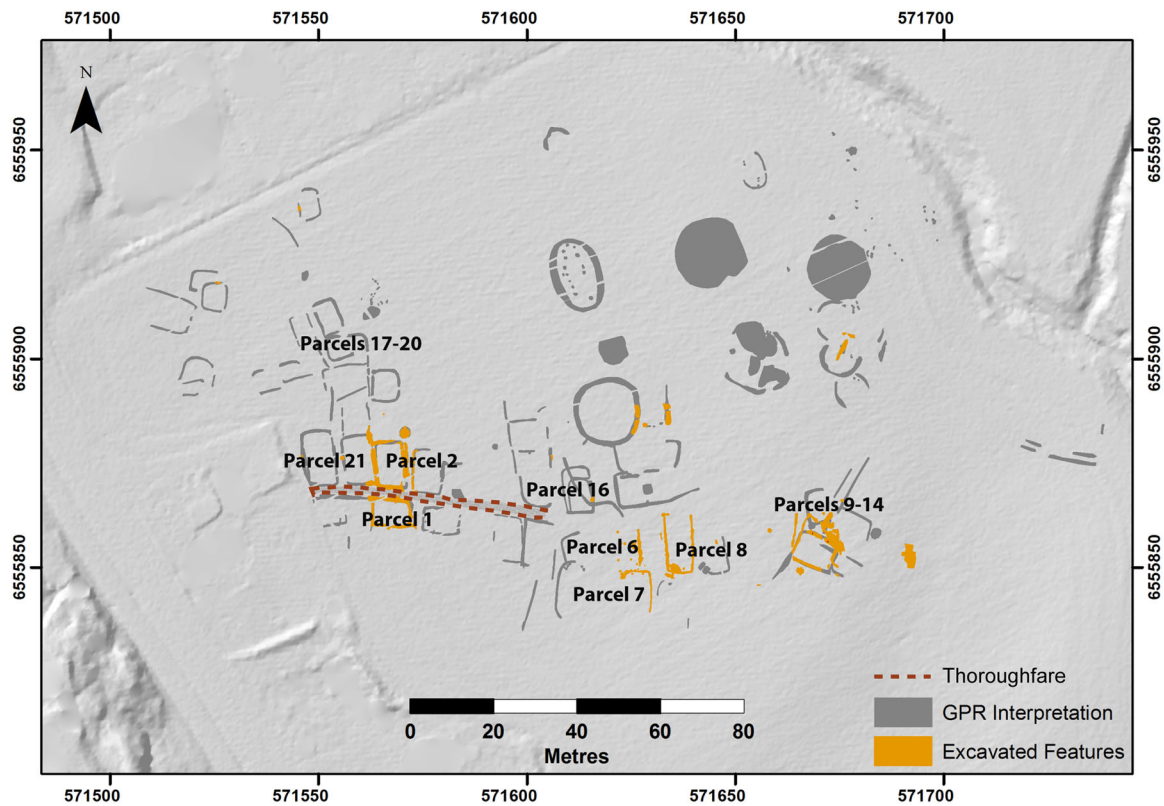
**FIGURE 2** The parcel ditches at Heimdalsjordet as identified via ground penetrating radar (dark grey shades) and excavation (lighter/yellow shades). The thoroughfare was poorly defined, and faded toward the east. The labeled parcel ditches are referred to in the text. Map Source: Norwegian Mapping Authority, Geovekst, and Municipalities 2020 [Color figure can be viewed at wileyonlinelibrary.com]

Henningsmoen, Høeg, Stabell, & Bukholm, 2007). The marine sediments are silty clay, with interspersed layers of sand deposited in a low energy coastal environment eventually progressing toward estuarine, intertidal conditions (Macphail, Crowther, & Linderholm, 2014; Schneidhofer et al., 2017). Located on the seaward side of the nearby and contemporary Gokstad Mound, the Heimdalsjordet site is currently at 3–6 m a.s.l., dating the emergence from the sea to c. 400–900 A.D. (Sørensen et al., 2007). The sea is now ca. 1 km distant; however, the site was located on the then coastline in the Viking Age. The land immediately surrounding the site is today a flat plain between exposed, steeply graded bedrock hills, the majority under 100 m a.s.l. The land has been levelled significantly by modern land use, from a gently undulating landscape intersected by small, entrenched streams, to a highly managed and drained agricultural landscape.

The area is composed of hydromorphic soils, predominantly stagnosols, with albeluvisols concentrated nearer current or former stream beds, as shown in Figure 3 (NIBIO, 2018). These soils are characterized by poor surface drainage and redoximorphic properties in the case of statgnosols, and despite the extensive drainage systems in the area, standing surface water occurs periodically on the site. Albeluvisols are also hydromorphic soils, classified by the translocation of clays down profile. Those located in the research area are Epistagnic Albeluvisols, indicating they also have impeded surface drainage (F.A.O, 2006; NIBIO, 2018; Solbakken, Nyborg, Sperstad, Fadnes, &

Klakegg, 2006). The hindered drainage could have reduced the past productivity of the land for cereal farming in the low lying areas, although it is more than suited to pasture, and sedge-grassland has been proposed for the area based upon the micromorphology evidence from preserved turfs in the nearby Gokstad Mound (Macphail, Bill, Cannell, Linderholm, & Rødsrud, 2013; Macphail et al., 2014).

Over the eastern part of the site, an area of sandy substrate overlies the gleyed marine clay silt, on which parcels 9–14 sit. This is the remains of a sand spit formed during postglacial sea level retreat. Composed of moderately sorted fine to coarse sands, it thins from south to north, and is intersected by a later stream bed which is now drained and infilled (see also Schneidhofer et al., 2017). Soils formed over this sand spit are classified as Haplic Arenosols, that is free draining sorted sandy soils, although this classification is generalized; in areas excavated the sand coverage over the marine silty clay is less than 1 m in depth, frequently less than 50 cm.

## 2 | METHODS

### 2.1 | GPR survey

Commissioned by the GOREV project, the wider geophysical landscape survey was conducted by ZAMG ArcheoProspections©, the
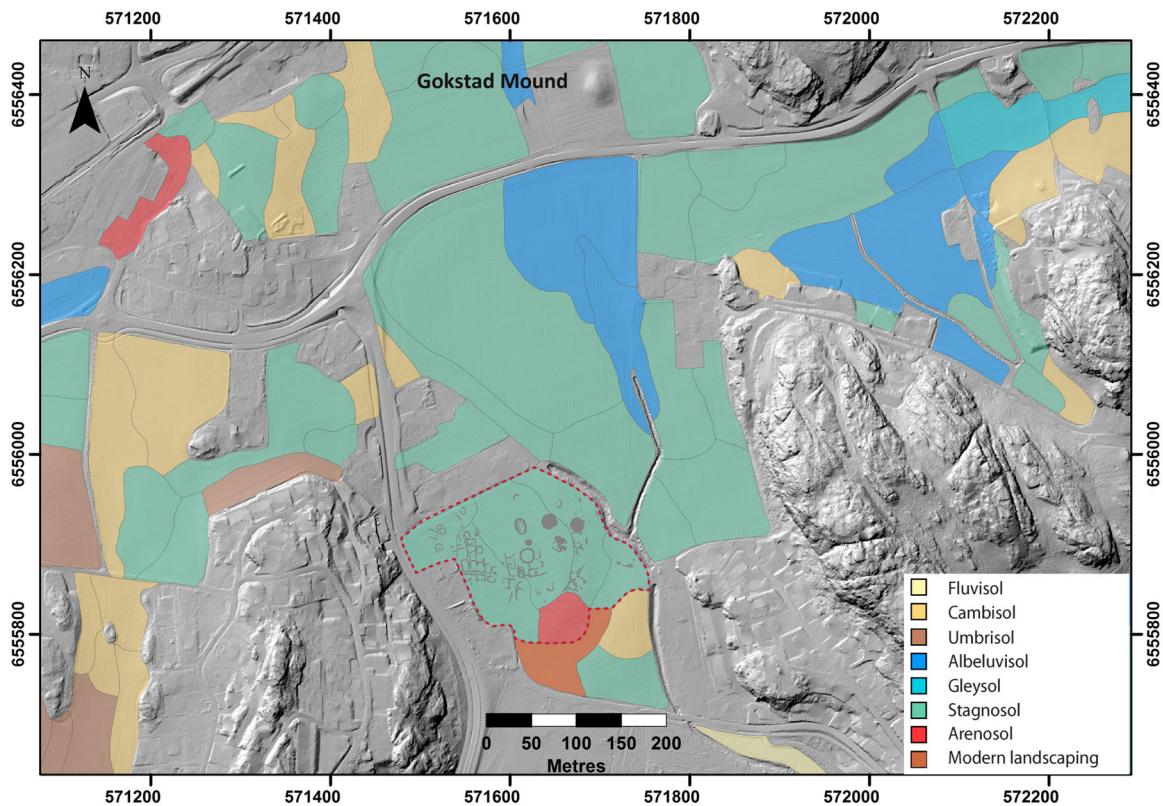
**FIGURE 3** Soil map showing the main categories of soil in the Heimdalsjordet area, based on the WRB system of classification (F.A.O, 2006). The case study site is outlined with a dashed line. To the north is the Gokstad Mound. Background is a hillshade model from LiDAR data. Please note that areas without colors referred to in the key are not currently classified. Map Source: NIBIO/Norwegian Mapping Authority, Geovekst, and Municipalities 2020 [Color figure can be viewed at wileyonlinelibrary.com]

Vienna Institute for Archaeological Science (VIAS), and their collaborative partners. The GPR survey encompassed 454 ha of land, centered on the Gokstad Mound. The data used for this study were produced using a 16-channel MÅLA MIRA array with 8 cm in-line and cross-line spacing, using 400 MHz antennas, pushed by a small tractor while using a GNSS real-time kinematic positioning system that had a 5 Hz position update rates. GPR data were first processed using ApRadar software (ZAMG ArcheoProspections©/LBI ArchPro) for trace interpolation, time-zero corrections, band-pass frequency filtering, spike removal, de-wow filters, average-trace-removal, amplitude-gain corrections, amplitude balancing, and Hilbert transformation (Schneidhofer et al., 2017; Trinks et al., 2018). The subsequent data set was then subject to visual filtering to enhance various aspects of the data set for interpretation. This study employs only a small area of this larger survey, which formed the basis for landscape analysis for archaeological and paleoenvironmental research by Schneidhofer et al. (2017).

## 2.2 | Coring

Cores were taken using a manual Eikelkjamp soil corer for hard soils, which takes undisturbed cores in a single use clear plastic liner, each measuring 300 mm in length, with a 49 mm diameter, with a 50 mm

cutting head. Cores were taken into the B horizon where it appeared devoid of archaeological material of interest, unless the core was specifically taken to sample the soil conditions. In these few cases, the core was taken into the C horizon (up to 2.35 m in depth).

From the area mechanically stripped of topsoil for the excavation in parcels 1, 2, 6, and 9–14, 15 cores were taken from the exposed surface into the visible parcel ditches. This was after selected sections of the parcel ditches had been excavated, to confirm the nature of the archaeology. Locations were selected to be representative of the ditches composition, close to recorded sections, and avoiding the extensive modern drainage ditches.

Coring samples as prospection were taken where GPR data had identified similar features of interest (Figure 4a,b). In total, 12 cores were taken for prospection, and without exception, archaeological deposits similar to the excavated parcel ditches were identified in the prospection cores.

When coring excavated contexts or for background samples, the 300 mm core sections were entirely manageable. Coring for prospection was more challenging. As each core section was 300 mm with a 50 mm cutting head, and the topsoil depth varied, between c. 20 and 28 cm, averaging 26 cm, this resulted in the truncated archaeology below the topsoil being missed in the cores. Essentially it was gathered in the cutting head between cores, as in some parts the surviving archaeology was only a few centimetres thick. The solution
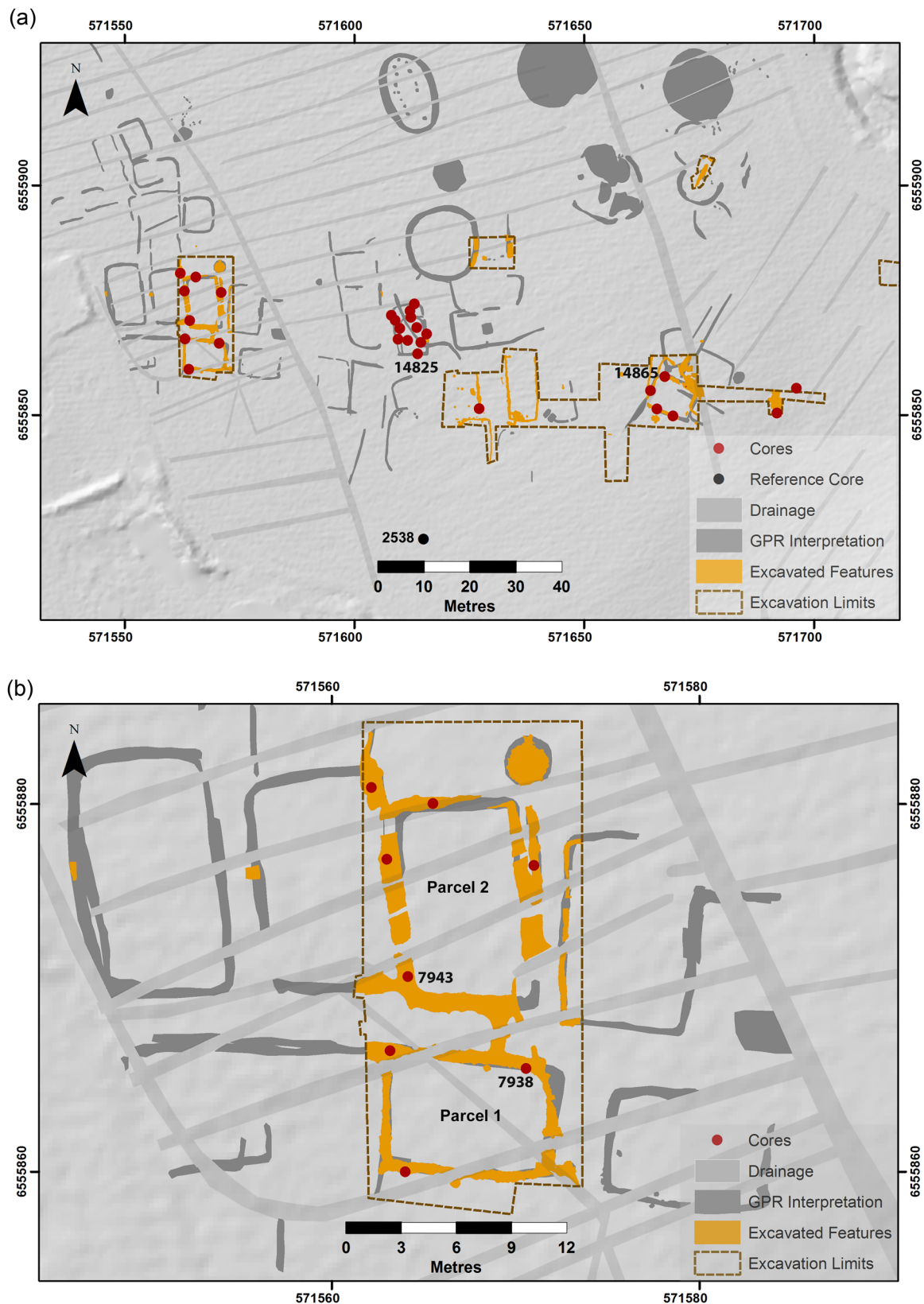
**FIGURE 4** (a) The location of cores taken in parcel ditches and used for geochemical analysis, with the cores illustrated and discussed in the text labeled by core number. The black marker to the south indicates the location of the background core taken in the vicinity of the Viking Age shoreline. The two cores to the east are located in the occupation layer associated with parcels 9–14. (b) An enhanced view of parcels one and two, with core locations in the topsoil stripped area marked. The modern drainage systems are also added to this figure to show the cutting of the parcel ditches. Map Source: Norwegian Mapping Authority, Geovekst, and Municipalities 2020 [Color figure can be viewed at wileyonlinelibrary.com]

## Core 2538

### Depth/elevation (m)     Layer Description

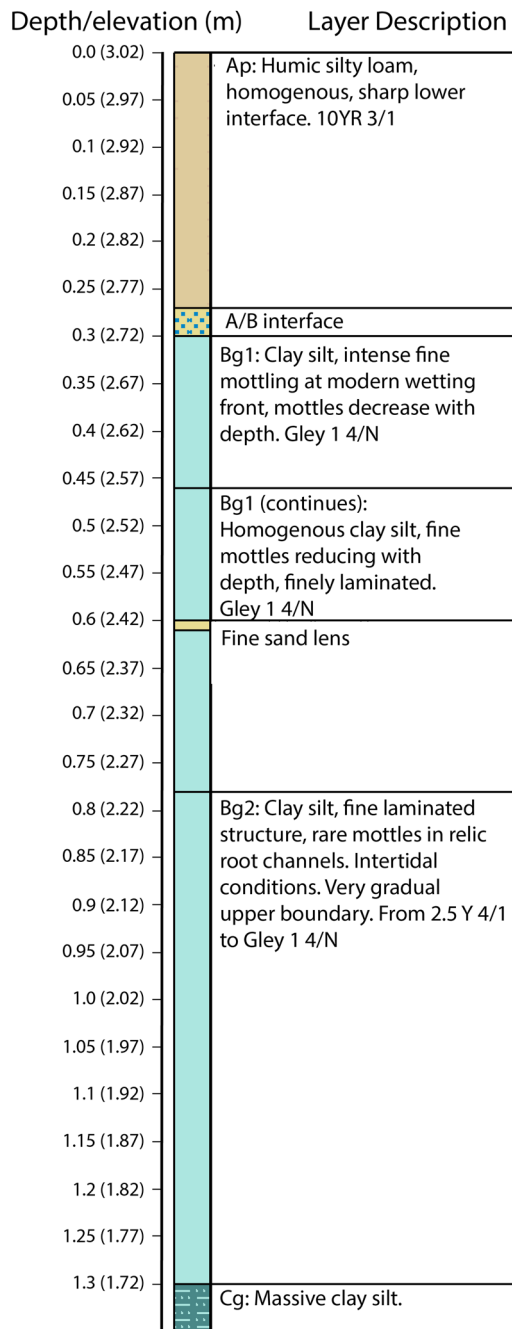| | |
|---|---|
| 0.0 (3.02) | **Ap:** Humic silty loam, homogenous, sharp lower interface. 10YR 3/1 |
| 0.05 (2.97) | |
| 0.1 (2.92) | |
| 0.15 (2.87) | |
| 0.2 (2.82) | |
| 0.25 (2.77) | |
| 0.3 (2.72) | A/B interface |
| 0.35 (2.67) | **Bg1:** Clay silt, intense fine mottling at modern wetting front, mottles decrease with depth. Gley 1 4/N |
| 0.4 (2.62) | |
| 0.45 (2.57) | |
| 0.5 (2.52) | **Bg1 (continues):** Homogenous clay silt, fine mottles reducing with depth, finely laminated. Gley 1 4/N |
| 0.55 (2.47) | |
| 0.6 (2.42) | Fine sand lens |
| 0.65 (2.37) | |
| 0.7 (2.32) | |
| 0.75 (2.27) | |
| 0.8 (2.22) | **Bg2:** Clay silt, fine laminated structure, rare mottles in relic root channels. Intertidal conditions. Very gradual upper boundary. From 2.5 Y 4/1 to Gley 1 4/N |
| 0.85 (2.17) | |
| 0.9 (2.12) | |
| 0.95 (2.07) | |
| 1.0 (2.02) | |
| 1.05 (1.97) | |
| 1.1 (1.92) | |
| 1.15 (1.87) | |
| 1.2 (1.82) | |
| 1.25 (1.77) | |
| 1.3 (1.72) | **Cg:** Massive clay silt. |

**FIGURE 5** Core 2538, the reference core as indicated in Figure 4a, with major horizons briefly described for texture and Munsell color. The core is 1.3 m long [Color figure can be viewed at wileyonlinelibrary.com]

was to core the first 10–15 cm of the topsoil and remove this before continuing the core. The result was that the uppermost 15 cm of topsoil was missing, leaving in the region of 10 cm of the lower topsoil for sampling. The process was applied to parcels 16 and 17–20, although parcels 17–20 proved to be too disturbed and truncated to be used for analysis.

## 2.3 | Background sampling

Middleton and Price (1996) suggested that, ideally, an off-site horizon should be found that is contemporary to and similar in properties to the measured archaeological horizon, and free from anthropogenic influence, which could then be measured for background values. Finding such an elusive soil while working in intensity cultivated land, is near impossible. Therefore, a core from the located Viking Age shoreline (ca. 3 m a.s.l.) was subsampled on all major horizons to use as rough guide control samples (Figures 4a and 5). This produced some broad geochemical parameters for the marine-sourced sediments which form the soil's parent material, which were used as a guide only. As many of the cores included subsoil sections, these provided the most relevant comparison material for the anthropogenic layers, as they represent the local conditions and could also capture the degree of translocation of geochemical signatures from the above archaeology. This data was incorporated into the statistical analysis. Issues such as leaching and disturbance which can have affected these subsoil samples are considered in the data analyses.

## 2.4 | Laboratory analysis

Once opened, the 27 selected cores were cleaned using a sharp, clean blade to remove surface smearing from the coring process, before being photographed and recorded for soil texture, Munsell color, archaeological and pedological stratigraphy, and inclusions such as archaeological finds or charcoal. In analysis and description, the archaeological stratigraphy was used to ensure integration with the archaeological interpretations.

The instrument used for elemental analysis was a Niton Xlt3 GOLDD[1] with a silver anode 50 kV, 0–200 μA X-ray tube. The selected mode was mining Cu/Zn, a four beam mode, with a total time per samples of 300 s. The limits of detection (LOD) was set to 2σ. Standard/certified reference materials (SRM hereafter) NIST 1646a, NIST 2711a, Sigma-Aldrich Trace Metals Clay 2 and Sigma-Aldrich Trace Metals Loamy Clay 2 were used throughout, after 10 or less samples, together with an analytical blank. Filter/beam times were selected from incremental increases on samples and SRMs (Cannell, 2017).

Before analysis, a 6 μm polypropylene X-ray film was placed between the instrument and sample point to keep the instrument window clean. The instrument was handheld for the direct core analysis, the instrument steadied against the core to ensure even contact. Cores were analysed at 2 cm intervals in archaeological contexts, and 4 cm intervals in topsoil and subsoil contexts, the distance measured from the top of the core using a manual ruler. Repeats were taken where readings suggested an error had occurred, and at random points to verify repeatability. Subsamples were taken from selected cores after direct analysis to verify differences in

---

[1]Geometrically optimized large area drift detector.

values and error as a result of sample processing. All data used for interpretation was calibrated to the SRM data, although the method of analysis renders the data semiquantitative at best.

## 2.5 | Data processing

Data was processed using IBM SPSS 23, Rockworks 15 by Rockware, and Microsoft Excel. The data set consisted of 374 sample points. These were classed according to stratigraphic horizon, under three broad categories of topsoil (T, *n* = 54), subsoil (S, *n* = 89) and archaeology/anthropogenic (A, *n* = 231). Categories subsoil (S) and topsoil (T) were also grouped as nonarchaeological (N). In addition, based upon interpretations from excavation records and observations in cores supplemented by comprehensive micromorphology data (Macphail et al., 2014), archaeological horizons were classed into early (E, *n* = 74) or late (L, *n* = 116) phases of occupation. The phasing only included sample points where micromorphology or stratigraphical observation could support phasing interpretations, on a parcel by parcel basis (Macphail et al., 2014; Macphail et al., 2016). The creation of subgroups within the geochemical data set was to allow parametric testing of groups to validate interpretations. Eighteen elements were selected for parametric testing. The initial selection criteria being those elements that could be calibrated, and produced significant results (over LOD set to 2$\sigma$), and subsequently elements were selected where previous experience and published research suggested they could be interpreted as potentially the result of past anthropogenic activity (e.g., Cannell, Cheetham, & Welham, 2017; Cook et al., 2005; Entwistle et al., 1998, 2000; Knudson, Frink, Hoffman, & Price, 2004; Middleton, 1996; Oonk et al., 2009; Wilson et al., 2008). The resulting data sets of 6,732 measured values (374 sample points for 18 elements) were then subjected to statistical analysis.

Before proceeding to principal component analysis (PCA), a one-tailed analysis of variance (ANOVA) test with A/N as a dependant variable was performed. The result (*F* 5.187, 0.000 significance value) confirmed there was significant variation between the archaeological and nonarchaeological soils. While some elements had a normal distribution, others, particularly metals such as Cu, Pb, and Ag, were skewed. Pearson's correlation (two-tailed) was used; however, this assumes a normal distribution of the data. To compensate, in tandem, bootstrapping was performed on all data, and separately on the topsoil only data set. This was done as the lower sample number (*n* = 54) meant that there was a degree of uncertainty in whether the PCA results for this data set were significant (see below). Bootstrapping does not assume normal distribution, and can be used to test the robustness of correlations identified via other statistical tests.

All data was then standardized (Z score) before covariance PCA analysis. PCA is sensitive to outliers/extreme values, which are reduced via standardization. Varimax rotation was selected as the data has a few dominant component loadings, such as those connected to soil structure, and some far smaller, which include zero values (e.g., Sn and Ag). A nonrotated data set is also simultaneously produced to verify interpretations (Abdi, 2003; Abdi & Williams, 2010).

The standardized data set was then tested in classified groups (topsoil = T, archaeology = A, subsoil = S, see above) To discern leaching into the subsoil, modern contamination of topsoil, archaeological horizons, and how effectively PCA could isolate soil processes and past human activity. The number of components considered significant was determined as four by scree plot (Abdi & Williams, 2010); although in all cases all eigenvalues over 0.8 were extracted. Further geostatistical analysis to relate localized enhancement of the interpreted factors/principal components was not done as the data are unsuitable.

To verify that PCA on each of the data sets would produce valid results for interpretation, a Kaiser–Meyer–Olkin measure of sampling adequacy was performed on both the standardized data set as a whole, and the topsoil only data set. The results were similar, with 0.726 for the whole data set, and 0.717 for the topsoil only. Results between 0.6 and 1 are seen as suggesting the variance within the data set is not random chance, but significant and suitable for PCA.

## 3 | RESULTS

Within Tables 1–4 values over ±0.5 are highlighted, with greater interpretive weight placed on higher values. Table 1 contains the whole data set, whereas Tables 2–4 show the results from the same data set separated into stratigraphic components (A, S, and T). The data are treated as a product of anthropogenic influences, soil processes and the analytical method, and is interpreted as such in the next section.

## 3.1 | Soil processes

### 3.1.1 | Sesquioxides/hydromorphic processes

In Tables 1–4, the correlation of iron (Fe), chromium (Cr), and vanadium (V) combining in a dimension is interpreted as the soil's sesquioxide component, and accounts for between 16.3% and 19.5% of the variation in the data set(s). In all but the topsoil, manganese (Mn) also has an affinity with these elements. Vanadium is common, albeit in far lower proportions, in Fe (hydr)oxides, as in soils the soluble $H_2VO_{4-}$ readily sorbs onto Mn, aluminum (Al), and Fe oxides, and thus often correlates with Fe. Where phosphorous (P) content is high, this can reduce V sorption, as phosphate can out-compete V in anion exchange and sorption in soils (Larsson, 2014), although how V is retained in soils is pH and redox dependent (Gäbler, Glüh, Bahr, & Utermann, 2009). Manganese and Fe are affected by cycles of reducing and oxidation in soils, which results in a leaching or redistribution of the these elements as they become soluble and are redeposited locally or more widely in oxidizing conditions such as root channels, voids or as the water table fluctuates (Birkeland, 1999). Sesquioxides or amorphous clay minerals, are common in tropical conditions where weathering is rapid (Tan, 1994), but also to a lesser extent, in acidic soils where clays are leached of their Si content. In these conditions, Al, Fe, and often Mn,

**TABLE 1** Results for Varimax rotated principal component analysis for all standardized data from cores ($n$ = 374)

| | Dimension | | | | | |
|---|---|---|---|---|---|---|
| **All** | **1** | **2** | **3** | **4** | **5** | **6** |
| Influence (%) | 25.3 | 16.4 | 16.3 | 10.4 | 6.1 | 5.4 |
| ZSn | −0.059 | 0.217 | 0.032 | 0.011 | 0.076 | 0.926 |
| ZAg | −0.001 | 0.038 | 0.017 | 0.034 | 0.942 | 0.086 |
| ZSr | 0.197 | −0.066 | −0.153 | 0.760 | −0.065 | 0.028 |
| ZRb | 0.716 | −0.135 | 0.178 | 0.148 | 0.008 | −0.102 |
| ZPb | −0.116 | 0.950 | 0.009 | 0.016 | −0.007 | 0.112 |
| ZZn | −0.093 | 0.421 | 0.425 | 0.013 | 0.331 | −0.222 |
| ZCu | −0.142 | 0.945 | 0.015 | 0.016 | 0.017 | 0.123 |
| ZFe | 0.056 | 0.110 | 0.899 | −0.069 | 0.035 | 0.021 |
| ZMn | −0.097 | −0.161 | 0.772 | 0.275 | −0.190 | 0.072 |
| ZCr | 0.478 | 0.088 | 0.714 | −0.149 | 0.162 | −0.042 |
| ZV | 0.467 | 0.081 | 0.795 | −0.228 | 0.094 | −0.001 |
| ZTi | 0.878 | −0.159 | 0.195 | −0.034 | 0.009 | −0.062 |
| ZCa | 0.093 | 0.028 | 0.070 | 0.858 | 0.084 | 0.009 |
| ZK | 0.920 | −0.157 | 0.132 | −0.003 | −0.026 | −0.028 |
| ZAl | 0.930 | −0.073 | 0.118 | 0.071 | 0.033 | 0.025 |
| ZP | −0.546 | 0.316 | 0.032 | 0.558 | 0.049 | −0.093 |
| ZSi | 0.793 | −0.213 | −0.276 | 0.237 | −0.073 | 0.076 |
| ZS | −0.291 | 0.808 | 0.063 | −0.005 | 0.059 | 0.061 |
| Interpretation | Clay/soil matrix | Nonferrous metalworking | Sesquioxides/hydromorphic processes | Organic waste | Silver | Tin |

*Note:* The "Z" indicates Z score value.

form metal oxides, typically $Al_2O_3$, $Fe_2O_3$, $Mn_2O$, although other forms occur and proportions vary (Mayer, Prietzel, & Krouse, 2001). In reducing conditions, $Mn_2O$ is reduced to the cation $Mn^{2+}$, which is in turn rapidly seized by Fe (hydr)oxides. Therefore, they remain correlated, as this sorption tends to remain stable until very low pH levels (He, Shentu, & Yang, 2010). In the plowed, aerated and relatively drained topsoil, Mn does not correlate with Fe, probably because of the lack of reducing conditions (Table 3). This could also be the uptake by plants, as Mn is generally found in far lower amounts compared to Fe (typically Fe 2–6%, Mn 0.03–0.1%), and is an essential plant nutrient (Brady & Weil, 1999). In these conditions, Cr forms a part of the factor as Mn is an oxidant, and is strongly retained in soils (Covelo, Vega, & Andrade, 2007; Ma & Hooda, 2010). Titanium (Ti), which correlates with Fe in the topsoil, also readily forms the metal oxide $TiO_2$, although this is not strictly speaking a sesquioxide (De Vos & Tarvainen, 2006).

### 3.1.2 | Clay minerals and modern agricultural inputs

Unsurprisingly, this component dominates the variation in the data set(s), accounting for up to 25.3% of the variation. The combination of silicon (Si) and Al is immediately recognizable as inherited minerals and layered clays, which in all data sets correlate with potassium (K) and Ti. Titanium is solely from minerogenic inputs and has no known biological function, indicative that this factor represents the soil's geogenic mineral components (Kylander, Ampel, Wohlfarth, & Veres, 2011). Interestingly, in all but the topsoil rubidium (Rb) also forms this factor (Tables 1, 2, and 4). Measured in proportions generally between 70 and 160 ppm, Rb, in the form of $Rb^+$, is assumed to be isomorphic substitutions in the clay lattice or a weathering product from K–Rb rich mica and feldspars. As Rb has similar atomic radii to K, it is a common substitution in the clay lattice, and is also found in similar quantities as those measured as a weathering product in southern Norway (De Vos & Tarvainen, 2006).

In the topsoil, Rb and strontium (Sr) correlate with P in dimension 4, whereas Ca and K correlate in dimension 3 (Table 3). This is assumed to be a combination of plow erosion bringing archaeological material into the topsoil, and modern additions from atmospheric inputs and artificial fertilizers adding to the organic and mineral components in the soil. Common micronutrients in fertilizers include copper (Cu), Fe, Mn, molybdenum (Mo), and zinc (Zn), as well as P (Brady & Weil, 1999). This could also explain dimension 5 in the

**TABLE 2** Results for Varimax rotated principal component analysis for standardized data from cores, archaeological layers only (*n* = 231)

| Archaeology | Dimension 1 | 2 | 3 | 4 | 5 | 6 |
|---|---|---|---|---|---|---|
| Influence (%) | 24.7 | 17.6 | 16.6 | 9.7 | 6.3 | 5.5 |
| ZSn | −0.055 | 0.206 | 0.037 | −0.005 | 0.074 | 0.936 |
| ZAg | −0.003 | 0.039 | 0.034 | 0.011 | 0.926 | 0.084 |
| ZSr | 0.299 | −0.104 | −0.108 | 0.718 | −0.107 | −0.011 |
| ZRb | 0.678 | −0.155 | 0.137 | 0.137 | −0.017 | −0.104 |
| ZPb | −0.148 | 0.950 | 0.007 | −0.013 | −0.022 | 0.112 |
| ZZn | −0.212 | 0.458 | 0.344 | 0.122 | 0.330 | −0.186 |
| ZCu | −0.183 | 0.945 | 0.005 | −0.016 | 0.000 | 0.124 |
| ZFe | −0.054 | 0.134 | 0.895 | −0.046 | 0.021 | 0.018 |
| ZMn | −0.197 | −0.170 | 0.736 | 0.268 | −0.232 | 0.067 |
| ZCr | 0.442 | 0.120 | 0.766 | −0.082 | 0.218 | −0.049 |
| ZV | 0.385 | 0.115 | 0.850 | −0.142 | 0.125 | 0.013 |
| ZTi | 0.864 | −0.159 | 0.189 | −0.024 | 0.038 | −0.081 |
| ZCa | 0.046 | 0.030 | 0.062 | 0.874 | 0.098 | 0.014 |
| ZK | 0.913 | −0.170 | 0.049 | 0.001 | −0.028 | −0.018 |
| ZAl | 0.923 | −0.066 | 0.075 | 0.100 | 0.032 | 0.043 |
| ZP | −0.570 | 0.318 | 0.015 | 0.529 | 0.048 | −0.067 |
| ZSi | 0.767 | −0.228 | −0.342 | 0.208 | −0.093 | 0.086 |
| ZS | −0.222 | 0.893 | 0.132 | −0.012 | 0.088 | 0.077 |
| Interpretation | Clay/soil matrix | Nonferrous metalworking | Sesquioxides/hydromorphic processes | Organic waste | Silver | Tin |

*Note:* The "Z" indicates *Z* score value.

topsoil as Zn alone. Unfortunately, the type and use of modern fertilizers on the site is not known, but certain fertilizers are a source of accumulating Zn, and of course other elements utilized by plants (Stacey, McLaughlin, & Hettiarachchi, 2010). Zinc can be from several sources, and it appears in background and subsoil samples where it is tentatively interpreted as marine-sourced (Tables 4 and 6; De Vos & Tarvainen, 2006). From the range of values for Zn, anthropogenic inputs in the parcel ditch backfills are modestly enhanced over subsoil levels of Zn, and are interpreted as human inputs without a clear source (Table 5). Zinc has been associated with bone material and general human occupation (Entwistle, et al. 1998; Ottaway & Matthews, 1988).

## 3.2 | Anthropogenic

### 3.2.1 | Organic waste

The correlation between Ca, Sr, and to a lesser extent P, accounts for 9.4–10.4% of the variation in the data in the archaeology and subsoil data sets (Tables 2 and 4), but differs in the topsoil. Just as the topsoil

samples are from directly over the archaeology, samples for the subsoil are largely taken within 15 cm of an archaeological deposit above, and therefore, dimensions 3 and 4 in Table 4 are possibly leaching and precipitation of metals and alkaline earth metals from archaeological contexts. In soils it is common for Ca and Sr to correlate. The similar atomic radii of Sr and Ca mean the less abundant Sr is a common substitution for Ca in rocks and minerals, and is easily weathered into solution in the mildly acidic conditions at Heimdalsjordet. For Ca, the mean and standard deviation (*SD*) of observations in the topsoil and subsoil differs from the archaeological contexts (Tables 5 to 7). For subsoil, the mean is 8,899.34 ppm and the SD 1,692.69 ppm, whereas for topsoil the mean is 8,836.61 ppm with a *SD* of 1052.74 ppm. The SD is less for topsoil, despite the similar averages. In the archaeological contexts, the figures are 10,527.60 ppm for the mean and 3,329.99 ppm for the *SD*. Despite the issue of comparing one data set with a larger number of observations to another with less, it does appear that the topsoil has least variation, whereas the archaeology is generally enhanced in Ca. For Sr, all horizons have a *SD* between 31 and 38 ppm, and the mean is slightly higher in the archaeology (181.98 ppm) compared to the topsoil (174.81 ppm) and the subsoil (158.60 ppm). These figures are

**TABLE 3** Results for Varimax rotated principal component analysis for standardized data from cores, topsoil layers only (n = 54)

| Topsoil | Dimension | | | | | |
| --- | --- | --- | --- | --- | --- | --- |
| | 1 | 2 | 3 | 4 | 5 | 6 |
| Influence (%) | 19.5 | 16.7 | 16.4 | 14.7 | 9.6 | 8.8 |
| ZSn | 0.262 | 0.092 | −0.141 | 0.049 | 0.039 | 0.871 |
| ZSr | 0.101 | 0.124 | 0.081 | 0.839 | −0.127 | 0.126 |
| ZRb | 0.029 | 0.159 | 0.103 | 0.810 | 0.069 | −0.448 |
| ZPb | 0.037 | −0.306 | −0.726 | 0.015 | 0.283 | 0.340 |
| ZZn | 0.349 | −0.115 | 0.016 | 0.036 | 0.814 | 0.065 |
| ZCu | 0.229 | −0.272 | −0.754 | −0.032 | 0.280 | 0.380 |
| ZFe | 0.875 | −0.021 | 0.227 | 0.107 | 0.206 | 0.097 |
| ZMn | 0.165 | 0.183 | 0.801 | 0.345 | 0.155 | 0.235 |
| ZCr | 0.918 | 0.129 | −0.006 | 0.171 | −0.004 | 0.119 |
| ZV | 0.912 | 0.226 | −0.125 | −0.132 | 0.048 | 0.099 |
| ZTi | 0.550 | 0.566 | 0.274 | 0.262 | −0.003 | 0.058 |
| ZCa | 0.341 | 0.435 | 0.639 | −0.164 | −0.213 | −0.046 |
| ZK | 0.218 | 0.592 | 0.511 | 0.275 | −0.138 | −0.373 |
| ZAl | 0.325 | 0.882 | 0.242 | 0.008 | −0.067 | −0.008 |
| ZP | 0.031 | −0.097 | 0.004 | 0.876 | −0.007 | 0.093 |
| ZSi | −0.055 | 0.922 | 0.246 | 0.028 | −0.156 | 0.095 |
| ZS | 0.103 | 0.104 | 0.277 | 0.122 | −0.786 | −0.003 |
| Interpretation | Sesquioxides/ Hydromorphic processes | Clay/soil matrix | Disturbed archaeology fertilizers | | Zinc (fertilizer/ disturbed archaeology) | Tin (disturbed archaeology) |

*Note:* The "Z" indicates Z score value.

close to the regional Sr levels (De Vos & Tarvainen, 2006) but it is probable Ca and Sr represent more than one input. The fact that Sr and Ca do not correlate in the topsoil by any test undertaken can perhaps be attributed to modern land use practices to reduce acidification, although the exact modern additions to the land are unknown at present.

That they do correlate in the subsoil and archaeological contexts is perhaps another issue. The affinity of Ca and Sr mean that from the geogenic inputs, they will correlate, even though Sr is far less plentiful than Ca. Calcium is enhanced in the archaeological contexts due to the additional inputs of Ca rich material, namely bone material and ash. This does not strongly correlate with P, the other main input from bone material, as P is present in virtually all other organic materials. However, they do correlate somewhat in the archaeological contexts. In the moderately acidic conditions at Heimdalsjordet, burnt bone was leached and weathered but still present, whereas unburnt bone has decomposed, the Ca and P released into the soil solution is retained in different forms and by different mechanisms. For Ca, commonly the cation $Ca^+$ is adsorbed onto clay surfaces and humic compounds, or leached into solution and lost to the soil (Brady & Weil, 1999). In occupation contexts, ash is also a

source of Ca. Mechanical and chemical weathering in these conditions will remove all traces over time (Canti, 2003; Courty, Goldberg, & Macphail, 1989), however, rare exceptions can occur if the deposit form allows by creating a more neutral microenvironment that reduces chemical loss, such as in urban "dark earth" contexts (Courty et al., 1989). The localized enhancements of Ca raise this as a possibility (Figure 6). Phosphorous, as part of anion exchange, in acidic conditions can form insoluble compounds with sesquioxides (Brady & Weil, 1999). In the archaeological data set, besides the correlation with Ca, that is bone and other organic human waste, it has no other correlation. Therefore bone and similar organic material from anthropogenic activity is the most likely source.

### 3.2.2 | Metal working

The final dimension(s) in each of Tables 1–4 are dominated by a single element; tin (Sn) or silver (Ag), and in one case, Zn. The data are no longer being reduced by PCA. In this case, these account for well under 10% of the variation. Therefore, undue weight will not be laid upon these data, although it deserves a mention as it is repeated

**TABLE 4** Results for Varimax rotated principal component analysis for standardized data from cores, subsoil layers only (*n* = 89)

| Subsoil | Dimension | | | | | |
|---|---|---|---|---|---|---|
| | **1** | **2** | **3** | **4** | **5** | **6** |
| Influence (%) | 23.1 | 17.2 | 15.1 | 11.4 | 9.5 | 6.4 |
| ZSn | −0.003 | −0.119 | 0.078 | 0.101 | 0.044 | 0.944 |
| ZSr | 0.308 | −0.137 | 0.747 | −0.064 | 0.290 | −0.089 |
| ZRb | 0.713 | 0.150 | −0.025 | −0.149 | −0.442 | −0.182 |
| ZPb | −0.012 | 0.192 | 0.147 | 0.886 | −0.012 | 0.001 |
| ZZn | −0.019 | 0.150 | −0.769 | −0.008 | 0.338 | −0.235 |
| ZCu | 0.034 | 0.050 | −0.215 | 0.906 | −0.028 | 0.134 |
| ZFe | −0.136 | 0.896 | −0.074 | 0.060 | −0.022 | −0.036 |
| ZMn | −0.005 | 0.749 | 0.327 | 0.386 | −0.106 | −0.092 |
| ZCr | 0.253 | 0.728 | −0.278 | −0.013 | 0.149 | −0.083 |
| ZV | 0.340 | 0.778 | −0.382 | 0.089 | −0.012 | −0.052 |
| ZTi | 0.878 | 0.084 | 0.243 | 0.068 | −0.184 | −0.083 |
| ZCa | 0.360 | −0.061 | 0.852 | −0.003 | 0.197 | 0.003 |
| ZK | 0.839 | 0.275 | 0.183 | −0.110 | −0.314 | −0.046 |
| ZAl | 0.912 | 0.037 | 0.059 | 0.052 | −0.019 | 0.084 |
| ZP | −0.327 | −0.180 | 0.210 | 0.122 | 0.761 | 0.096 |
| ZSi | 0.737 | −0.296 | 0.393 | 0.157 | 0.042 | 0.198 |
| ZS | −0.212 | 0.318 | −0.053 | −0.264 | 0.659 | −0.047 |
| Interpretation | Clay/soil matrix | Sesquioxides/ hydromorphic processes | Leaching | Leaching | Organic matter, reducing conditions | Tin (leaching?) |

*Note:* The "Z" indicates Z score value.

in each of the data sets. The other anthropogenic metals, Cu and Lead (Pb), are also considered here as evidence for nonferrous metal working. In Table 5, and Tables 8 and 9, the enhancement of metals such as Cu, Pb, Sn, and Ag is clearly connected to the archaeological levels, and the later phase of activity on the site. Figures 7 and 8 also illustrate that these enhancements can be highly localized.

Tin (Sn) behaves differently to the other metals commonly exploited by past human populations. In natural conditions, Sn is either in the form of $Sn^{2+}$ or $Sn^{4+}$, the latter being iron-loving, the prior even more selective. Tin forms few minerals, cassiterite ($SnO_2$) being the dominant form, although minerals with Cu and sulfur (S) also occur (Kabata-Pendias, 2010, pp. 337–338). Silver has several mineral forms with other elements; however, in naturally occurring minerals form, Ag is often argentite, $Ag_2S$, or native silver, Ag. Silver has the strongest affinities to S and chlorine (Cl), although in these organic and slightly acidic soils, S is comparatively abundant, whereas Cl is only detected in close proximity to bone material. With S, in organic or inorganic forms, Ag forms strong bonds, which can and do out-compete many other common metal cations, such as $Cu^+$ and $Pb^+$, attracted to colloid surfaces (Evans & Barabash, 2010). The principal component with Ag alone as a dominant influence can,

therefore, be interpreted as a product of the low proportion of silver within the samples, its concentration in a few specific contexts, and its strong retention in these conditions through colloidal adsorption with S. Similarly, Sn is found in low to medium concentrations in few contexts, and is commonly found in soils, either as a cation, or in mineral form with O.

As mentioned previously, S is fairly abundant. Sulfur is generally associated with wetter conditions, reducing environments and the organic soil fraction; however, it is also in mineral form in complexes with metal ions. Sulfur is found in plant material, marine-sourced sediments and geological formations, although in soil it is usually in organic forms. Within the organic fraction it is fairly stable, but once released/weathered as ions, it is easily leached (White, 2006). In reducing conditions, bacteria release S into the soil matrix in anion form, although in Fe and sesquioxide rich soils, such as at Heimdalsjordet, sulfate can be adsorbed and retained (Tan, 1994, 1998).

Returning to the data tables, as noted above, $Ag_2S$ is a common form of silver. Sulfur does not correlate well with Ag, because of the difference in abundance and the universally anthropogenic source for Ag, whereas S will be to some degree also naturally occurring. In the data presented, sulfur correlates differently in the topsoil,

**TABLE 5** Descriptive statistics for the archaeology levels (A) from the geochemical core data

| A only | Sn | Sr | Rb | Pb | Zn | Cu |
|---|---|---|---|---|---|---|
| N | 231 | 231 | 231 | 231 | 231 | 231 |
| Mean | 10.98 | 181.98 | 112.11 | 98.52 | 74.10 | 120.99 |
| SD | 75.75 | 31.44 | 18.49 | 537.12 | 20.94 | 497.64 |
| Minimum | 0.00 | 85.90 | 54.04 | 0.00 | 27.51 | 0.00 |
| Maximum | 1,084.34 | 301.70 | 161.87 | 6,473.32 | 171.13 | 5,518.56 |
| Sum | 2,535.69 | 42,038.17 | 25,897.95 | 22,758.53 | 17,117.09 | 27,949.33 |
| A only | Fe | Mn | Cr | V | Ti | Ca |
| N | 231 | 231 | 231 | 231 | 231 | 231 |
| Mean | 28,012.12 | 460.15 | 56.43 | 84.31 | 3,588.52 | 10,527.60 |
| SD | 11,875.16 | 265.51 | 15.37 | 25.41 | 731.50 | 3,329.99 |
| Minimum | 11,428.09 | 165.96 | 0.00 | 22.79 | 1,256.08 | 5,524.63 |
| Maximum | 111,544.87 | 2,628.87 | 95.90 | 169.44 | 5,357.52 | 48,975.61 |
| Sum | 6,470,799.92 | 106,295.40 | 13,035.66 | 19,476.57 | 828,948.70 | 2,431,874.59 |
| A only | K | Al | P | Si | S | Ag |
| N | 231 | 231 | 231 | 231 | 231 | 231 |
| Mean | 19,874.81 | 35,899.31 | 1,915.45 | 202,170.80 | 341.98 | 0.32 |
| SD | 3,712.87 | 10,646.29 | 1,720.40 | 41,130.42 | 289.01 | 2.61 |
| Minimum | 8,323.58 | 11,727.10 | 244.27 | 64,049.50 | 45.62 | 0.00 |
| Maximum | 36,076.43 | 72,881.84 | 12,559.64 | 306,133.19 | 3,003.90 | 34.38 |
| Sum | 4,591,080.10 | 8,292,740.49 | 442,468.45 | 46,701,454.94 | 78,996.57 | 75.01 |

*Note:* All data is in ppm, with the exception of N (no. of samples).

archaeology and subsoil layers. Indeed in the topsoil, it does not correlate with much at all, although the bootstrap testing weakly correlated it with the clay matrix minerals Al, K, Si as well as Mn and Ca. In the archaeological horizons, S forms a principal component with Pb and Cu. In the subsoil, it correlates with P. The most common form of S in soils is the bacterially formed pyrite ($FeS_2$), although other mineral forms are known, such as the previously mentioned $Ag_2S$, and other Fe bearing mineral forms (Kabata-Pendias, 2010; Mees & Stoops, 2010). In the site conditions, S is likely to form stable sulfides with other metallic ions, such as $Cu^{2+}$. Lead also has an affinity for S, and these forms for both Cu and Pb are fairly insoluble and unavailable for plant uptake (Hough, 2010). If the soil drains, some forms of metallic sulfides become oxidized and more soluble (Kabata-Pendias, 2010), which explains the presence of Cu and Pb in the upper subsoil horizons as leached. Together, this implies that the principal component in the archaeological contexts where Pb, Cu and S correlate is a result of organic and metal inputs from anthropogenic activity being subject to intermittent reducing conditions since deposition. This is highly plausible in hydromorphic soils. Many of the concentrations of nonferrous metals are in contexts with gleyed characteristics, including primary and secondary Fe mottles and coatings.

### 3.3 | Results by phase

The phase results are only considered in terms of descriptive statistics on the calibrated data (Tables 8 and 9). The cut off between the early (E) and late (L) phase is based upon elemental values, micromorphology results, and excavation records, and is imperfect in that the cores do not necessarily represent the same features and layers that were recorded during excavation. Visually, the cores contained more anthropogenic-sourced inclusions in the later phase, such as burnt clay, bone, and charcoal, which was also distinguishable by the geochemical measured values. An early phase with less anthropogenic waste and less variation in the waste can therefore be compared to the later phase, where inputs suggest a wider range of activities and thus inputs, and considerably more intense.

Of note, when considering the differences between the phases, is that the mean and SD for the elements extracted as anthropogenic from PCA analysis are enhanced to varying degrees. For example, Ca is only slightly enhanced in late phase (Table 9) compared to the early (Table 5), yet the SD is over twice that of the early phase. In Figures 6–9, the lighter shades define the contexts interpreted as belonging to the later phase, and corresponds to the peaks in Ca, Sr, P, Cu, Pb, and S. Conversely, the darker shades relate to contexts

**TABLE 6** Descriptive statistics for the subsoil levels (S) from the geochemical core data

| S only | Sn | Sr | Rb | Pb | Zn | Cu |
| --- | --- | --- | --- | --- | --- | --- |
| N | 89 | 89 | 89 | 89 | 89 | 89 |
| Mean | 0.38 | 158.60 | 115.39 | 15.49 | 74.57 | 31.73 |
| SD | 3.61 | 37.66 | 12.37 | 13.25 | 14.36 | 20.22 |
| Minimum | 0.00 | 112.71 | 5.67 | 5.67 | 32.25 | 0.00 |
| Maximum | 34.09 | 391.23 | 103.27 | 103.27 | 114.72 | 129.31 |
| Sum | 34.09 | 14,115.57 | 10,269.69 | 1,378.66 | 6,636.95 | 2,824.28 |
| S only | Fe | Mn | Cr | V | Ti | Ca |
| N | 89 | 89 | 89 | 89 | 89 | 89 |
| Mean | 31,780.12 | 472.77 | 68.69 | 105.79 | 4,064.87 | 8,899.34 |
| SD | 8,113.59 | 137.02 | 12.41 | 19.55 | 456.42 | 1,692.69 |
| Minimum | 14,875.22 | 319.54 | 35.96 | 51.51 | 3,012.12 | 6,169.23 |
| Maximum | 65,931.97 | 1,113.63 | 109.17 | 147.93 | 5,707.22 | 14,199.62 |
| Sum | 2,828,430.83 | 42,076.92 | 6,113.54 | 9,415.04 | 361,773.20 | 792,041.14 |
| S only | K | Al | P | Si | S | Ag |
| N | 89 | 89 | 89 | 89 | 89 | 89 |
| Mean | 22,140.13 | 40,743.00 | 980.53 | 208,165.17 | 319.30 | 0.00 |
| SD | 2,501.52 | 7,495.21 | 387.16 | 30,628.14 | 169.68 | 0.00 |
| Minimum | 16,101.28 | 24,462.44 | 398.75 | 142,231.33 | 75.25 | 0.00 |
| Maximum | 30,749.02 | 69,382.23 | 2,129.00 | 334,704.78 | 1,078.27 | 0.00 |
| Sum | 1,970,471.56 | 3,626,127.00 | 87,267.45 | 18,526,700.22 | 28,418.10 | 0.00 |

*Note:* All data is in ppm, with the exception of N (no. of samples).

belonging to the early phase, where these elements are less enhanced. For P, both the mean and *SD* increase markedly in the later phase (Tables 8 and 9). From the low sum and mean, it is clear the nonferrous metals are far rarer in the early phase. As these phase divisions are using stratigraphic context boundaries, this can be interpreted as that nonferrous metalworking, almost exclusively, is a later phase phenomenon. Silver can be seen as a minor contribution to the evidence of nonferrous metalworking in the parcel ditch backfills. Elements associated with the soil matrix, such as Si and Rb, decrease slightly in the later phase as proportionately the archaeological sediments are more organic and thus marginally less minerogenic.

## 3.4 | Cores

On a core-by-core basis, a broader, meso-scale picture can be gathered. Within Figures 6–9 besides the selected cores and elemental values, are regression scores from the PCA analysis, constructed from the Z score data using the PCA results. Each regression score is a standardized score for the data at that sample point, for each dimension. The scores are between −3 and +9 in this case. A negative score means this point/sample has less than average influence on the principal component, and a positive score means it has a more than average influence. Thus, the higher the score, the more concentrated the geochemical causes of each principal component are in that sample/context. It also follows that principal component regression scores with the greater value range have more extreme values, and thus are more influenced by localized concentrations. This is particularly the case for the anthropogenic factors identified via PCA.

One activity that was clearly localized was nonferrous metal working. In core 14825 (Figures 4a and 7), there is peak of 6,473 ppm Pb, and core 7938 (Figures 4b and 8) contains a peak of 11,556 ppm Pb; the highest values measured in the cores. Covariance between Pb, Cu, Sn, Zn, and the presence of Ag can be observed in the cores in Figures 7 and 8, suggesting metal working at or near these locations. On a core-by-core basis, these peaks are also concentrated in cores taken close to the thoroughfare.

Above the general enhancement of organic material from settlement, as indicated by P and Ca, the episodic nature of the organic deposits is also apparent in the occasional but marked peaks in the organic waste dimension. Similarly, the fluctuations in the soil matrix dimension indicates episodes of in-washing from precipitation or flood events, as is evidenced in the micromorphology data (Macphail et al., 2016). These were also apparent in the cores themselves as laminated deposits of coarser material with charcoal flecks, often

**TABLE 7** Descriptive statistics for the topsoil (T) from the geochemical core data

| T only | Sn | Sr | Rb | Pb | Zn | Cu |
|---|---|---|---|---|---|---|
| N | 54 | 54 | 54 | 54 | 54 | 54 |
| Mean | 9.86 | 174.81 | 91.39 | 71.24 | 61.76 | 74.24 |
| SD | 15.27 | 33.78 | 11.33 | 38.82 | 8.64 | 49.99 |
| Minimum | 0.00 | 101.08 | 75.79 | 13.76 | 37.48 | 0.00 |
| Maximum | 73.71 | 286.35 | 154.86 | 164.23 | 80.93 | 237.41 |
| Sum | 532.18 | 9,439.50 | 4,935.18 | 3,847.17 | 3,335.10 | 4,009.00 |
| **T only** | **Fe** | **Mn** | **Cr** | **V** | **Ti** | **Ca** |
| N | 54 | 54 | 54 | 54 | 54 | 54 |
| Mean | 20,649.97 | 340.79 | 45.47 | 65.72 | 3,088.23 | 8,836.61 |
| SD | 3,333.85 | 60.64 | 16.12 | 10.89 | 261.00 | 1,052.74 |
| Minimum | 16,428.36 | 188.28 | 32.22 | 51.68 | 2,597.95 | 5,755.80 |
| Maximum | 35,563.76 | 479.03 | 142.86 | 119.92 | 4,054.78 | 11,473.12 |
| Sum | 1,115,098.25 | 18,402.83 | 2,455.63 | 3,549.08 | 166,764.19 | 477,176.98 |
| **T only** | **K** | **Al** | **P** | **Si** | **S** | **Ag** |
| N | 54 | 54 | 54 | 54 | 54 | 54 |
| Mean | 16,038.84 | 25,083.50 | 2135.92 | 172,013.04 | 547.42 | 0.00 |
| SD | 1,516.56 | 3,436.10 | 912.13 | 15,522.99 | 167.06 | 0.00 |
| Minimum | 13,456.29 | 15,495.76 | 1,115.76 | 131,904.24 | 382.96 | 0.00 |
| Maximum | 19,539.90 | 31,871.85 | 7,491.00 | 202,646.30 | 1,410.26 | 0.00 |
| Sum | 866,097.55 | 1,354,509.09 | 115,339.66 | 9,288,704.05 | 29,560.89 | 0.00 |

*Note:* All data is in ppm, with the exception of N (no. of samples).

with an erosional lower boundary. The recutting of the parcel ditches could be seen in sections, and this has removed/disturbed phases. With the elements associated with organic waste, there is also a tendency for the highest concentrations to be found in the cores near the thoroughfare.

## 3.5 | Summary of interpretations

Clearly soil processes dominate, but here the task is to discriminate the anthropogenic enhancement within and above this. The combinations of Pb, Cu, and S, probably from sulfide ores, impurities in refined metals and/or organic inputs, are all measured at levels far above subsoil levels and background data (De Vos & Tarvainen, 2006). From the clear connection to the archaeological levels, and particulary the later phase of occupation, these are interpreted as evidence for nonferrous metalworking, without making the assumption this is the only source of enhancement. In the core data, these elements, as well as Ag and Sn, appear in concentrations on the horizontal and vertical planes (Figures 6–9). They do not correlate well in the PCA analysis as they are present in different concentrations, and retained and mobilized by different soil processes, entered the soil in different

forms, and plural forms probably exist at present; however, they are all highly likely to represent metalworking.

Human settlement increases organic inputs, which has caused the enhanced P and S. From the cores these increase in the later phase of the site, suggesting greater inputs. The enhancement of Ca and to a lesser extent Sr above the levels from modern land-use and geogenic inputs, is also attributed to human activity, including but not exclusively, ash and bone material.

From the distribution of the enhancement and correlation of the measured values, it is evident that the deposits contained localized inputs related to specific activities, such as metal working, and more generalized inputs from organic refuse from multiple sources. These accumulated in the ditches by differing acts of deposition, until the site becomes truncated by the plow.

## 4 | DISCUSSION

### 4.1 | Dealing with generalizations in three dimensions

Returning to secondary contexts from cores and in dealing with samples representing the vertical, horizontal and potentially
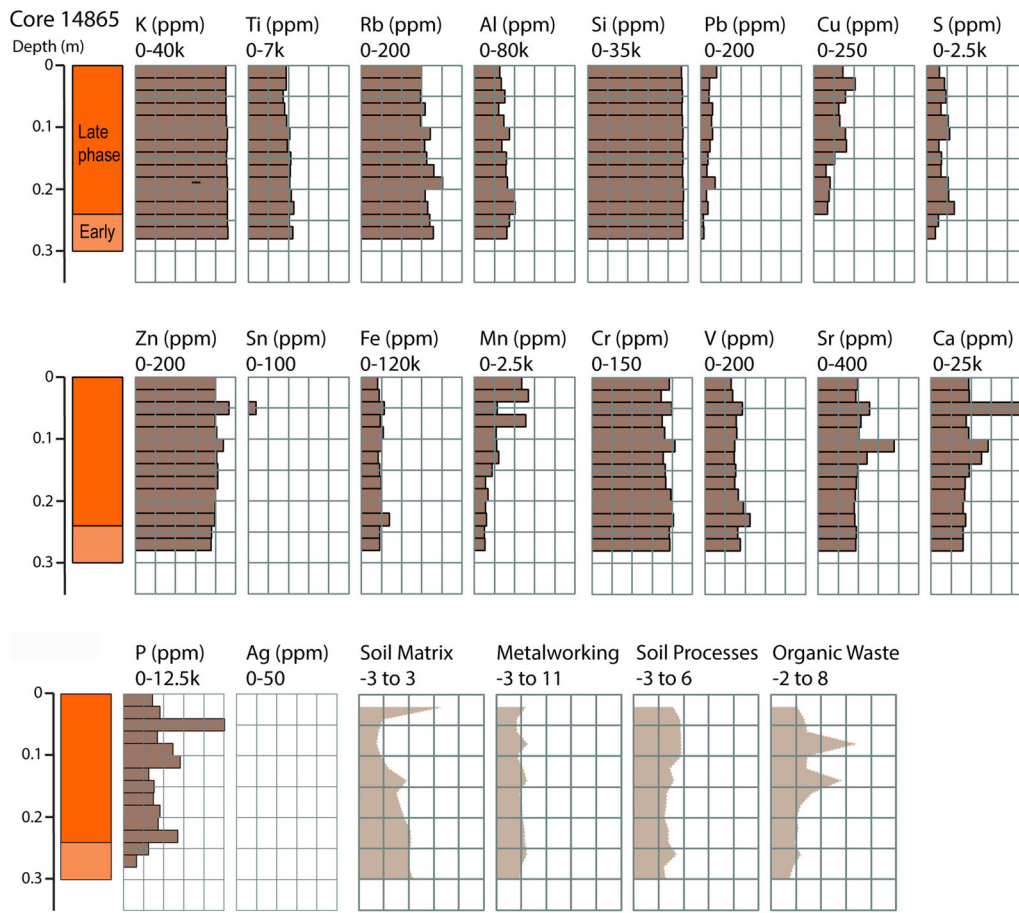
**FIGURE 6** Core 14865, parcel 9, with archaeological horizons only. In the core, darker/orange indicates the late phase, and lighter/peach indicates the early phase. There is no subsoil or topsoil in this core [Color figure can be viewed at wileyonlinelibrary.com]

chronological planes as part of the geochemical data set, interpretations cannot be made purely on archaeological terms. Time is represented both in the accumulation of matter, and the post depositional processes that have subsequently affected the deposits. To interpret this data set, the natural variation has to be explained in conjunction with the archaeological (Oonk et al., 2009; Oonk et al., 2009; Wilson et al., 2009). This is in part a product of the applied analytical method on truncated features, and that cores and secondary deposits can limit spatial interpretation. Statistical analysis coupled with the incorporation of samples from not just the archaeology, but also the adjacent topsoil and subsoil, has helped define natural processes and chronological processes, and also their inter-relationship. This makes the remaining archaeology less in terms of influence in the data set(s), but stronger in interpretative strength.

The flexibility and minimal sample preparation possible when using pXRF allows the capture of fine scale, three-dimensional stratigraphy from a large number of samples. This volume challenges our interpretative ability to make thorough use of the microscale. In general, the geochemical stratigraphy appears to match the physical divisions observed in the cores, although there are instances where it does not. For example, in core 14865, parcel 9 and Figure 6, there is an increase in organic waste, with P and Ca, which was not recorded

in the core stratigraphy. Here, both can be used to question or measure what they really represent in terms of what is mobile, and what is significant, because coring and geochemical analysis have not been widely applied in archaeology on this scale. The limited leaching into the subsoil appears to be consistent with soil properties, definable, and elementally selective, therefore, the geochemistry is recording variation in anthropogenic deposits otherwise challenging to detect at this scale.

## 4.2 | Relating values to inputs

It is fairly logical to assume the more input, the more trace remains there are to be measured. This assumption, however, does not hold for all elements in all soil conditions when time is added to the equation (Wilson et al., 2008). As an example, in acidic soils Ca, is easily leached (Brady & Weil, 1999; Ottaway & Matthews, 1988), which has in part resulted in the lack of unburnt bone and ash on the site. Another major constitute of bone, P, can quickly become stable in inorganic mineral form in these conditions, especially with Fe and Al oxides (Bethell & Máte, 1989; Linderholm, 2007), but as stated previously, P can be from multiple sources. Therefore, we cannot

**TABLE 8** Descriptive statistics for the early phase from the geochemical core data

| Early | Sn | Sr | Rb | Pb | Zn | Cu |
|---|---|---|---|---|---|---|
| N | 74 | 74 | 74 | 74 | 74 | 74 |
| Mean | 1.25 | 180.20 | 120.60 | 18.12 | 68.33 | 34.82 |
| SD | 9.60 | 27.94 | 18.39 | 13.53 | 13.25 | 24.92 |
| Minimum | 0.00 | 97.50 | 87.39 | 0.00 | 41.09 | 0.00 |
| Maximum | 82.14 | 232.88 | 159.61 | 82.41 | 106.48 | 153.68 |
| Sum | 92.22 | 13,334.95 | 8,924.45 | 1,340.81 | 5,056.53 | 2,576.60 |
| Early | Fe | Mn | Cr | V | Ti | Ca |
| N | 75 | 74 | 74 | 74 | 74 | 74 |
| Mean | 29,160.93 | 434.53 | 62.44 | 95.04 | 4,072.55 | 10,044.08 |
| SD | 9,400.40 | 110.97 | 15.00 | 24.65 | 636.26 | 1,977.42 |
| Minimum | 14,780.01 | 245.82 | 22.99 | 40.51 | 2,855.89 | 5,524.63 |
| Maximum | 51,015.38 | 780.08 | 93.43 | 146.01 | 5,357.52 | 16,128.53 |
| Sum | 2,187,069.55 | 32,155.24 | 4,620.74 | 7,033.27 | 301,368.92 | 743,261.98 |
| Early | K | Al | P | Si | S | |
| N | 74 | 74 | 74 | 74 | 74 | |
| Mean | 22,098.40 | 41,906.06 | 1,178.92 | 217,368.45 | 250.63 | |
| SD | 3,470.77 | 12,365.77 | 712.97 | 46,507.46 | 118.95 | |
| Minimum | 16,373.45 | 11,727.10 | 244.27 | 76,784.06 | 59.21 | |
| Maximum | 28,805.02 | 72,881.84 | 3,724.08 | 306,133.19 | 544.19 | |
| Sum | 1,635,281.83 | 3,101,048.60 | 87,240.07 | 16,085,264.94 | 18,546.38 | |

*Note:* All data is in ppm, with the exception of N (no. of samples).

equate any values directly with inputs in any quantitative proportion. What we *can* assume is intra-site comparability when the environmental conditions are more or less constant. From this, phases and/or intensity of inputs can be equated to settlement pattern or density.

Therefore, intensity, and by extension phase and change, can be measured in stratigraphic accumulation on an element grouping basis. Comparable studies, such as Wells et al. (2000), equated intense activity with high P values for middening, and high Hg and Pb values with craft production areas. Both Aston, Martin, and Jackson (1998) and Cook and Heizer (1965) attempted to equate the waste produced by humans and domestic species to the potential for detecting sites by relative enhancement, but both stopped short of equating measured values to physical input by direct correlation. They both consider it to be the proportional relative enhancement of groups of elements that suggest activity occurrence or focus and intensity. On an element by element basis, the measured values are both connected to inputs, preservation, and soil conditions over time.

Therefore, for the Heimdalsjordet site, the late phase is markedly different from the early. This is both in terms of inputs volume, and the activity range represented. The issue with this statement is time. None of the data presented here allow a time frame per phase to be estimated. Intensity can either be by duration, or intensity, the resulting volume is the same. Unfortunately, this is a limitation of geochemistry,

exacerbated by the truncated and secondary nature of the deposits. From using cores, the sequence of accumulation can be seen, but not necessarily whether it is intensity or duration that creates the enhancement. Here, we can turn to the finds, such as the bead assemblage, which suggest the main activity on the site was in the 9th and 10th centuries, and the radiocarbon dating (Bill & Rødsrud, 2017). These data suggests the site was used more intensely in the later period, however, this phase also has a longer duration. In addition, the later phases in the micromorphology data produced evidence of more intense inputs from human and animal waste, together with fragments such as leather, which were absent in the earlier phase (Macphail et al., 2016). Therefore, from the geochemistry perspective, the duration and intensity of this settlement phase creates the enhancement, as does its preservation. The earlier phase is perhaps shorter and less intense in the range of activity and the waste produced, but also truncated by later ditch digging (Bill & Rødsrud, 2017).

## 4.3 | Interpreting the scales and phases of heimdalsjordet

The parcel ditches and site topography show interesting similarities. It is clear that the majority of the ditches in form and formation were alike

**TABLE 9** Descriptive statistics for the late phase from the geochemical core data

| Late | Sn | Ag | Sr | Rb | Pb | Zn |
|---|---|---|---|---|---|---|
| N | 116 | 116 | 116 | 116 | 116 | 116 |
| Mean | 21.06 | 0.73 | 187.49 | 108.50 | 179.63 | 79.99 |
| SD | 105.88 | 3.88 | 35.60 | 18.73 | 750.68 | 24.10 |
| Minimum | 0.00 | 0.00 | 85.90 | 54.04 | 7.13 | 31.85 |
| Maximum | 1,084.34 | 34.38 | 301.70 | 161.87 | 6473.32 | 171.13 |
| Sum | 2,443.46 | 75.01 | 21,748.62 | 12,586.04 | 20,836.61 | 9,278.39 |
| Late | Cu | Fe | Mn | Cr | V | Ti |
| N | 116 | 116 | 116 | 116 | 116 | 116 |
| Mean | 209.17 | 28,178.06 | 476.39 | 53.63 | 79.06 | 3,316.50 |
| SD | 691.91 | 15,189.37 | 356.05 | 13.85 | 25.34 | 690.34 |
| Minimum | 0.00 | 11,428.09 | 165.96 | 25.11 | 23.11 | 1,256.08 |
| Maximum | 5,518.56 | 111,544.87 | 2,628.87 | 95.90 | 169.44 | 4,776.58 |
| Sum | 24,263.89 | 3,296,833.46 | 55,260.74 | 6,220.72 | 9,171.48 | 384,714.02 |
| Late | Ca | K | Al | P | Si | S |
| N | 116 | 116 | 116 | 116 | 116 | 116 |
| Mean | 10,988.05 | 18,246.16 | 32,388.65 | 2,458.77 | 192,956.70 | 380.22 |
| SD | 4,347.23 | 3,040.72 | 8,870.68 | 2,023.61 | 38,807.27 | 376.95 |
| Minimum | 5,634.79 | 8,323.58 | 13,111.33 | 364.43 | 64,049.50 | 45.62 |
| Maximum | 48,975.61 | 25,323.64 | 53,223.59 | 12,559.64 | 291,212.77 | 3,003.90 |
| Sum | 1,274,614.09 | 2,116,555.00 | 3,757,083.65 | 285,217.19 | 22,382,977.23 | 44,105.89 |

Note: All data is in ppm, with the exception of N (no. of samples).

and comparable. Almost all cores suggested the ditches had been recut, and to look at the GPR interpretations, many parceled areas have clearly phased ditch alignments and formations. With few exceptions, the alignment of the ditches remains with the thoroughfare, and the changes in size and alignment of the parceled areas, from what we can see, are minor. If we consider, from the finds and the ^{14}C dates (see Bill & Rødsrud, 2017), that the cores probably represent decades, if not more, then we have a conservative picture before us. This implies that space, in terms of plot/parcel location, ditch alignment and perhaps even activities, were maintained over generations of activity. However, in the context of late Iron Age Norway, trading sites and proto-urban settlements were also radical departure from the enduring settlement form of the longhouse and farmstead (Eriksen, 2015), and therefore, conservatism in settlement form must, in parallel, be seen in this context.

Using parcel 2 as an example, the illusive earliest phases with low level animal stocking and human occupation debris probably date to the very end of the 8th century or the start of the 9th (Macphail et al., 2014; Macphail et al., 2016). These deposits are truncated, and the next deposits mark a more intense occupation. Later ditch infilling in parcel 2 includes finds of rock crystal beads dated to A.D. 860–885 and/or 915–980 (Bill & Rødsrud, 2017; Callmer, 1977; Rødsrud, 2014), and other less chronologically distinct objects such as whetstones fragments, crucibles, copper alloy bars, and so forth.

None are in situ; none can be ascribed purpose other than loss or discard based upon stratigraphic observations. Then the parcel ditches are truncated again by the modern plow. It is likely, based on the ^{14}C dates and finds, that a larger proportion of the 9th century occupation is glimpsed in the ditches of parcel 2, perhaps even into the early 10th century (Bill & Rødsrud, 2017). Even if, as seems likely, the site continued in one form or another until the plundering of the Gokstad Mound sometime between A.D. 953 and 975, or even after (Bill & Daly, 2012; Bill & Rødsrud, 2017), there is nothing to say exactly when the relative chronology of parcel 2 becomes truncated.

To summarize what can be distinguished from the geochemical data, in parcels 1, 2, and 16, the thoroughfare was the focus throughout the occupation, as the gathering point for waste and activities. This seems to hold for all phases. Parcels 9–14 have high organic inputs (Figure 6), as illustrated by the enhancement of P values. Here is also where a disproportionate amount of weights were found, beside an area tentatively interpreted as a harbor or storage location. Perhaps this area functioned as a gateway for storage and exchange (Bill & Rødsrud, 2013; Macphail et al., 2014; Bill & Rødsrud, 2017). Nonferrous metalworking can be located in the vicinity of parcels 21 and 16, interestingly at exactly the same point in the parcels form; in close proximity to a ditch beside the thoroughfare. Indeed the base of a nonferrous metal working oven was
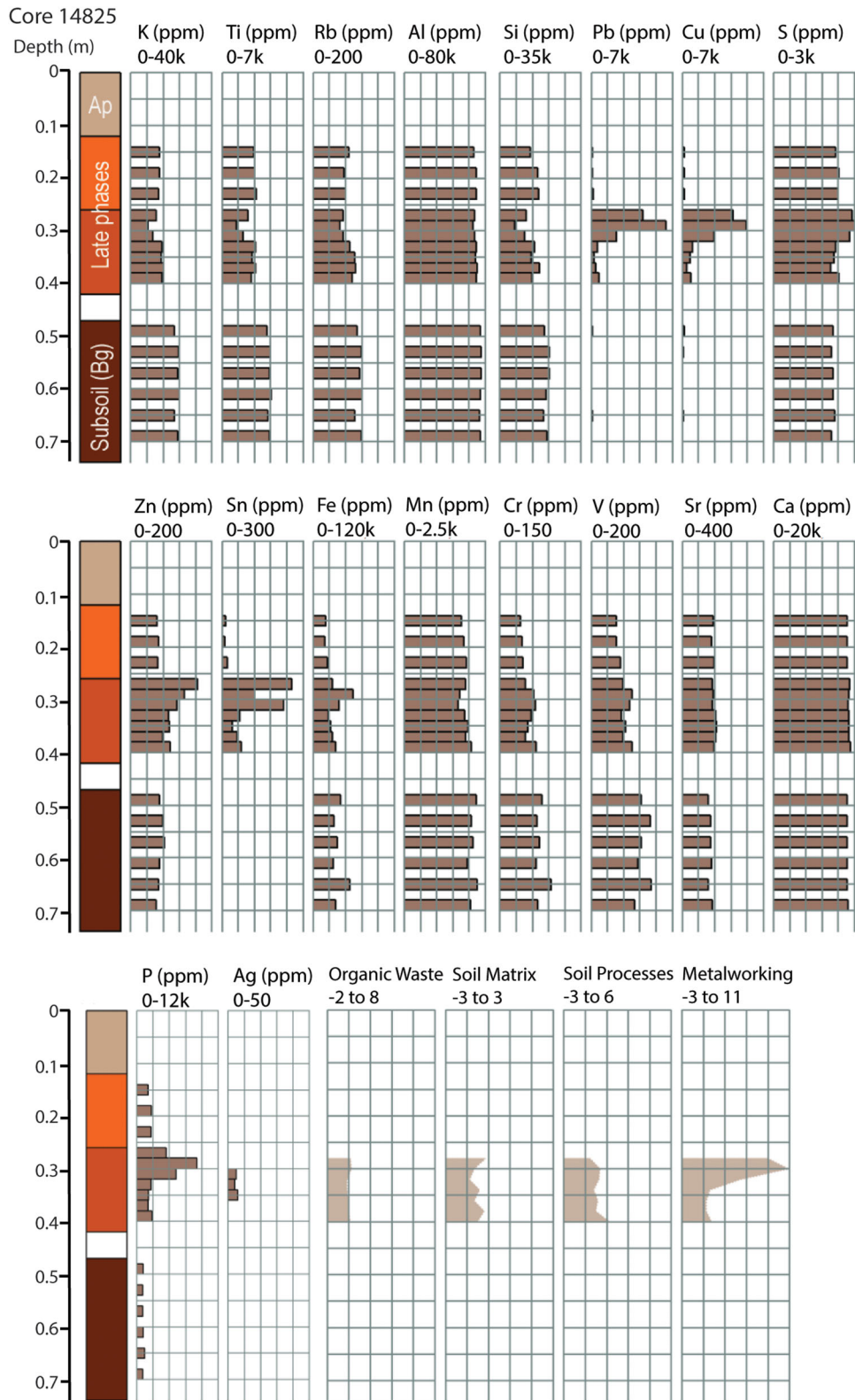
**FIGURE 7** Core 14825, parcel 16, with topsoil, archaeological and subsoil horizons. In the core, lightest shade/light brown represents topsoil, mid/orange shades indicate the late phase, and darker/brown is subsoil. The divisions within phases represent archaeological stratigraphy/contexts. The hiatus is the gap between cores caused by the cutting head [Color figure can be viewed at wileyonlinelibrary.com]
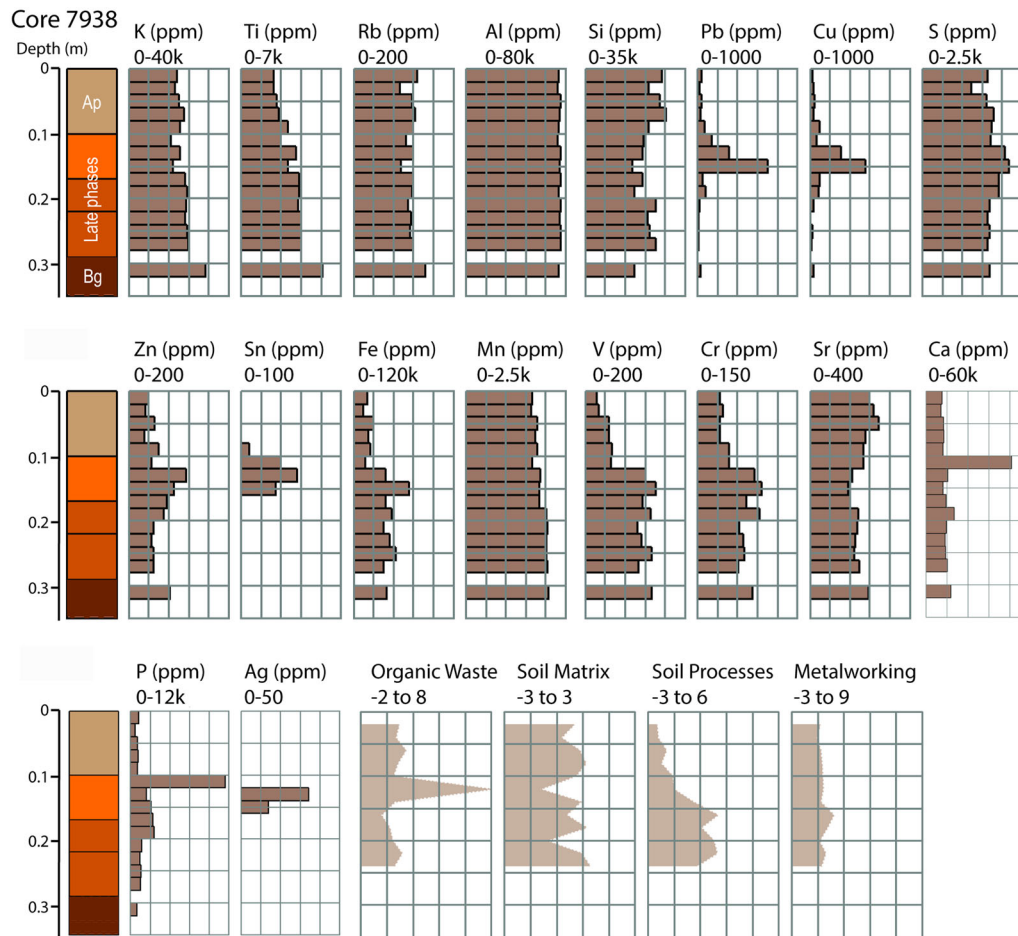
**FIGURE 8** Core 7938, parcel 1, with archaeological and subsoil horizons. In the core, lightest shade/light brown represents topsoil, mid/orange shades indicate the late phase, and light/peach is subsoil. The divisions within phases represent archaeological stratigraphy/contexts [Color figure can be viewed at wileyonlinelibrary.com]

located in the upper ditch fills of parcel 21 (see supporting information). Both also seem to have been used by people working with a range of nonferrous metals, including lead, silver, and copper alloys. Working in a ditch on a site prone to waterlogging would not be the most logical location, but this could be a product of preservation making the exception being perceived as the rule.

Within each parcel, excluding parcels 9–14 were the road is not present, there is spatial patterning relating to the relative enhancement. This spatial variation is far more distinct for the later phase. It appears the areas of greatest relative enhancement are nearest the thoroughfare, where the waste is focussed, which holds for both phases. This suggests that there is a "front" and a "back" to the plots/parcels, with activity producing waste focused on the front and the thoroughfare (Tuan, 1977).

## 4.4 | The methods potential

The three-dimensional approach, using geochemistry to capture the horizontal, vertical and relative chronological use of the space on a site

where only negative features remain, enhances our understanding of the range of activities on the site over time. By combining coring with geophysics, in this case high-resolution GPR data, the method can be expanded to include both excavated and unexcavated areas of a site. As applied to Heimdalsjordet, this methodology was entirely successful, in that every feature identified from the GPR interpretations was found by geo-referencing, cored and analysed. The implication has a very positive outlook for research and commercial archaeology, as many sites cannot be wholly excavated, even if they are under threat from development. The method can also be used to obtain prospection information before excavation to better plan fieldwork in relation to time and budget. At present, the data sets presented in this paper offer a far more nuanced picture of the functioning of Heimdalsjordet than would otherwise be obtainable, with chronological information connected to the intensification and increasing diversity of the settlement over time. On truncated sites, it is demonstrated here that when some spatial preservation is present, targeted geochemical sampling on secondary deposits can evidence the evolution of the site in terms of space and activity.

It is easy to lose sight of certain assumptions in archaeological geochemistry when the labels are made archaeological, and the
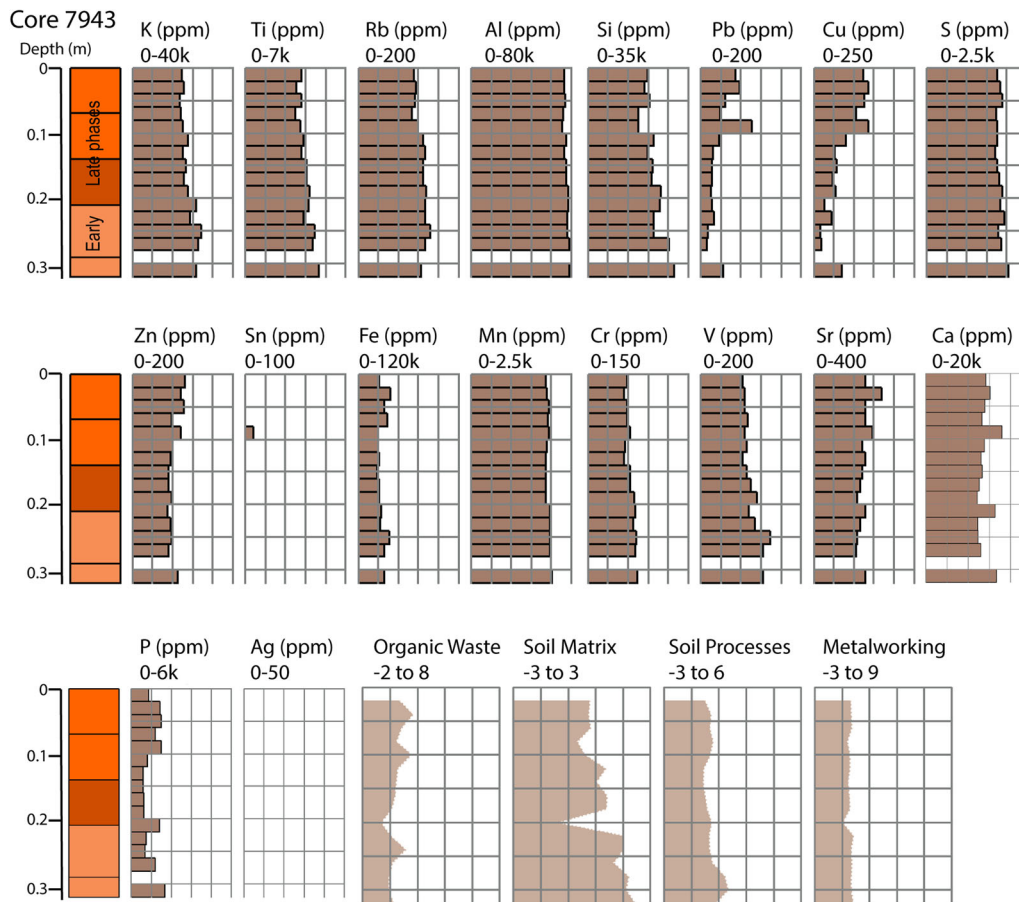
**FIGURE 9** Core 7943, parcel 2, showing archaeological layers only. In the core, the darker/orange shades indicate the late phase, and the lighter/peach shades indicate the early phases. The divisions within phases represent archaeological stratigraphy/contexts. There is no subsoil or topsoil in this core [Color figure can be viewed at wileyonlinelibrary.com]

interpretations related to archaeological features, human-made objects and how they all tie together in one big settlement picture. Geochemistry is essentially measuring the soil processes; its ability over time to breakdown and retain/redistribute organic and mineral inputs and disturbances. The time-frames archaeologists work on are generally superficial for soil formation, but still, the soil in all its organic and inorganic physical and chemical processes, will have decomposed, altered and utilized those inputs to some degree. The interpretations provided here, attempt to take this into account. This considered this study would have benefited from a broader range of complimentary data from analysis of the soils composition and variability off-site and on-site, which will be considered in future research.

## 5 | CONCLUSION

Considering the continued truncation of the site by plowing, the approach and resulting data presented here represents an attempt to harvest some spatial and chronological meaning from the site before erosion reduced the site further. Considering this, the GPR data used

in this study are highly unlikely to be bettered in terms capturing archaeological features that are rapidly vanishing. In the same vein, the geochemical data represent features that will soon be eroded away, and all potential data lost. The combination of coring, geophysics, and pXRF is cost effective and less invasive, and therefore, has potential beyond this case study, if the context and question are suitable. Many archaeological sites are under threat from plow erosion (Huisman, Heeres, van Os, Derickx, & Schoorl, 2016), and rapid and effective sampling techniques, such as cores, can be used as a basis for analysis, or an evaluation of the sites potential. It is clear from this case study that secondary deposits such as these are a valid and useful source of information on the use of space, how it changed over time from one phase to the next, and where the activity foci were. Applying pXRF directly to the cores allowed rapid analysis and subsequently a larger number of samples could be incorporated into the research, giving a broader spatial representation of the occupation on the site over time.

The limitation of the data set presented here is that, while clear from the statistical analysis, only two archaeological factors relating to past settlement could be readily defined. These were organic, bone-rich waste, and nonferrous metalworking. Raw amber was

found on the site, as was a fragment of leather, and these represent just a fraction of the many potential artisanal activities that occurred on the site using predominantly organic materials (Macphail et al., 2014; Rødsrud, 2014). To be able to capture more detail from the range of potential organic materials, either more directly related contexts are required for sampling, or a greater sample density and stratigraphic control is required, if not both. There is potential to more closely combine fine-stratigraphic geochemistry and micromorphology to help confirm the source of enhancement by micromorphology, and gain the distribution and thus use of space via geochemistry.

The ditches consistently show signs of recutting, and the high degree of truncation results in uncertainty over what these secondary deposits represent in both activity and chronological terms. These deposits are the result of slow accumulation, dumps, silting, and in-washing. They are both intentional and unintentional; the background to generations of settlement, and only a fraction thereof. It is all we have, and that is not unusual. Our mandate is to use this scant resource to maximum effect if it divulges a greater contextual understanding of the human past.

## DATA AVAILABILITY STATEMENT

The data that support the findings of this study are openly available in the eprints repository at Bournemouth University, available at http://eprints.bournemouth.ac.uk, reference number 29660.

## ORCID

*Rebecca J. S. Cannell* 🄳 http://orcid.org/0000-0001-7416-8189

## REFERENCES

Abdi, H. (2003). Factor rotations in factor analyses. In M. Lewis-Beck, A. Bryman & T. Futing (Eds.), *The SAGE encyclopedia for social science research methods* (pp. 792–795). Thousand Oaks, CA: Sage.

Abdi, H., & Williams, L. J. (2010). Principal component analysis. *Wiley Interdisciplinary Reviews: Computational Statistics, 2*, 433–459.

Aston, M. A., Martin, M. H., & Jackson, A. W. (1998). The potential for heavy metal soil analysis on low status archaeological sites at Shapwick, Somerset. *Antiquity, 72*(278), 838–847.

Bethell, P. H., & Máté, I. (1989). The use of soil phosphate analysis in archaeology: A critique. In J. Henderson (Ed.), *Scientific analysis in archaeology* (pp. 1–29). Oxford: Oxford Univeristy Committee for Archaeology.

Bethell, P. H., & Smith, J. U. (1989). Trace-element analysis of an inhumation from Sutton Hoo, using inductively coupled plasma emission spectrometry: An evaluation of the technique applied to analysis of organic residues. *Journal of Archaeological Science, 16*(1), 47–55.

Bill, J., & Daly, A. (2012). The plundering of the ship graves from Oseberg and Gokstad: An example of power politics? *Antiquity, 86*(333), 808–824.

Bill, J., & Rødsrud, C. L. (2013). En ny markeds-og produksjonsplass ved Gokstad i Vestfold. *Nicolay Arkeologisk tidsskrift, 120*, 5–12.

Bill, J., & Rødsrud, C. L. (2017). Heimdalsjordet: Trade, production and communication. In Z., Glørstad, T. & K. Loftsgarden (Eds.), *Viking-Age transformations* (pp. 212–231). Oxon: Routledge.

Birkeland, P. W. (1999). *Soils and geomorphology*. New York, NY: Oxford University Press.

Booth, A. D., Vandeginste, V., Pike, D., Abbey, R., Clark, R. A., Green, C. M., & Howland, N. (2017). Geochemical insight during archaeological geophysical exploration through in situ X-ray fluorescence spectrometry. *Archaeological Prospection, 24*(4), 361–372.

Brady, N. C., & Weil, R. R. (1999). *The nature and properties of soils* (12th ed.). New York, NY: Macmillan Publishing Company.

Callmer, J. (1977). *Trade beads and bead trade in Scandinavia ca. 800-1000 A.D.* Gleerup: Lund.

Cannell, R. J. S. (2017). *Prospecting the physicochemical past. Three dimensional geochemical investigation into the use of space in Viking Age sites in southern Norway using portable XRF* (Unpublished Thesis). Bournemouth University.

Cannell, R. J. S., Cheetham, P., & Welham, K. (2017). Geochemical analysis using portable X-ray fluorescence. In D. Skre (Ed.), *Avaldsnes—A sea-king's manor in first millennium Western Scandinavia* (pp. 421–454). Berlin/Boston, MA: Walter de Gruyter.

Canti, M. (2003). Aspects of the chemical and microscopic characteristics of plant ashes found in archaeological soils. *Catena, 54*, 339–361.

Carver, M. (1995). Digging for data: Principles and procedures for evaluation, excavation and post-excavation in towns. Dia. In W. S. Hensel, T. & P. Urbanczyk (Eds.), *Theory and practice of archaeological research 2: Acquisition of field data at multi-strata sites. Dialogue with the data: The archaeology of complex societies and its context in the 90's* (pp. 45–120). Warsaw: Institute of Archaeology and Ethnology, Polish Academy of Sciences.

Cook, D. E., Kovacevich, B., Beach, T., & Bishop, R. (2005). Deciphering the inorganic chemical record of ancient human activity using ICP-MS: A reconnaissance study of late Classic soil floors at Cancuen, Guatemala. *Journal of Archaeological Science, 33*(2006), 628–640.

Cook, S. F., & Heizer, R. F. (1965). Studies on the chemical analysis of archaeological sites. *Univerisity of Calafornia Publications in Anthropology, 2*, 1–102.

Cook, S. R., Banerjea, R. Y., Marshall, L., Fulford, M., Clarke, A., & van Zwieten, C. (2010). Concentrations of copper, zinc and lead as indicators of hearth usage at the Roman town of Calleva Atrebatum (Silchester, Hampshire, UK). *Journal of Archaeological Science, 37*(4), 871–879.

Cook, S. R., Clarke, A. S., & Fulford, M. G. (2005). Soil geochemistry and detection of early Roman precious metal and copper alloy working at the Roman town of Calleva Atrebatum (Silchester, Hampshire, UK). *Journal of Archaeological Science, 32*(5), 805–812.

Courty, M. A., Goldberg, P., & Macphail, R. I. (1989). *Soils and micromorphology in archaeology*. Cambridge: Cambridge University Press.

Couture, A., Bhiry, N., Monette, Y., & Woollett, J. (2016). A geochemical analysis of 18th-century Inuit communal house floors in northern Labrador. *Journal of Archaeological Science: Reports, 6*, 71–81.

Covelo, E. F., Vega, F. A., & Andrade, M. L. (2007). Competitive sorption and desorption of heavy metals by individual soil components. *Journal of Hazardous Materials*, *140*(1–2), 308–315.

Crowther, J. (1997). Soil phosphate surveys: Critical approaches to sampling, analysis and interpretation. *Archaeological Prospection*, *4*, 93–102.

De Vos, W., & Tarvainen, T. (2006). Elements Ag-Zr. In W. De Vos & T. Tarvainen (Eds.), *Geochemical atlas of Europe Part 2: Interpretations of geochemical maps, additional tables, figure, maps, and related publications* (Vol. 2). Geological Society of Finalnd.

Entwistle, J. A. (2000). The geoarchaeological significance and spatial variability of a range of physical and chemical soil properties from a former habitation site, Isle of Skye. *Journal of Archaeological Sciences*, *27*, 287–303.

Entwistle, J. A., & Abrahams, P. W. (1997). Multi-elemental analysis of soils and sediments from Scottish historical sites. The potential of inductively coupled plasma-mass spectrometry for rapid site investigation. *Journal of Archaeological Sciences*, *24*, 407–416.

Entwistle, J. A., Abrahams, P. W., & Dodgshon, R. A. (1998). Multi-element analysis of soils from Scottish historical sites. interpreting land-use history through the physical and geochemical analysis of soil. *Journal of Archaeological Sciences*, *25*(1), 53–68.

Entwistle, J. A., Dodgshon, R. A., & Abrahams, P. W. (2000). An investigation of former land-use activity through the physical and chemical analysis of soils from the Isle of Lewis, Outer Hebrides. *Archaeological Prospection*, *7*, 171–188.

Entwistle, J. A., Mccaffrey, K., & Abrahams, P. (2009). Three-dimensional (3D) visualisation: The application of terrestrial laser scanning in the investigation of historical Scottish farming townships. *Journal of Archaeological Sciences*, *36*, 860–866.

Eriksen, M. H. (2015). *Portals to the Past: An archaeology of doorways, dwellings, and ritual practice in Late Iron Age Scandinavia. Department of Archaeology, Conservation and History* (Unpublished Ph.D thesis). University of Oslo.

Evans, L. J., & Barabash, S. J. (2010). Molybdenum, silver, thallium and vanadium. In P. S. Hooda (Ed.), *Trace elements in soils* (pp. 515–551). Chichester: John Wiley & Sons/Blackwell Publishing.

F.A.O. (2006). World reference base for soil resources. In F.A.O (Ed.), *A framework for international classification, correlation and communication* (Vol. 103). Rome, Italy: United Nations.

Feveile, C. (2008). Ribe. In S. Brink & N. Price (Eds.), *The Viking World* (pp. 126–130). Oxon, UK/New York: Routledge.

Frahm, E. (2013a). Commentary: Is obsidian sourcing about geochemistry or archaeology? A reply to Speakman and Shackley. *Journal of Archaeological Sciences*, *40*, 1444–1448.

Gauss, R. K., Bátora, J., Nowaczinski, E., Rassmann, K., & Schukraft, G. (2013). The Early Bronze Age settlement of Fidvár, Vráble (Slovakia): Reconstructing prehistoric settlement patterns using portable XRF. *Journal of Archaeological Sciences*, *40*(7), 2942–2960.

Gäbler, H. E., Glüh, K., Bahr, A., & Utermann, J. (2009). Quantification of vanadium adsorption by German soils. *Journal of Geochemical Exploration*, *103*(1), 37–44.

Hayes, K. (2013). Parameters in the use of pXRF for archaeological site prospection: A case study at the Reaume Fort Site, Central Minnesota. *Journal of Archaeological Sciences*, *40*(8), 3193–3211.

He, Z. L., Shentu, J., & Yang, X. E. (2010). Mangenese and selinium. In P. S. Hooda (Ed.), *Trace elements in soils* (pp. 481–495). Chichester: John Wiley & Sons.

Holliday, V. T., & Gartner, W. G. (2007). Methods of soil P analysis in archaeology. *Journal of Archaeological Sciences*, *34*(2), 301–333.

Hough, R. L. (2010). Copper and lead. In P. S. Hooda (Ed.), *Trace elements in soils*. Chichester: John WIley & Sons/Blackwell Publishing.

Huisman, H., Heeres, G., van Os, B., Derickx, W., & Schoorl, J. (2016). Erosion and errors: Testing the use of repeated LIDAR analyses and erosion modelling for the assessment and prediction of erosion of archaeological sites? *Conservation and Management of Archaeological Sites*, *18*(1–3), 205–216.

Hunt, A., & Speakman, R. (2015). Portable XRF analysis of archaeological sediments and ceramics. *Journal of Archaeological Sciences*, *53*, 626–638.

Jones, R., Challands, A., French, C., Card, N., Downes, J., & Richards, C. (2010). Exploring the location and function of a Late Neolithic house at Crossiecrown, Orkney by geophysical, geochemical and soil micromorphological methods. *Archaeological Prospection*, *17*, 29–47.

Kabata-Pendias, A. (2010). *Trace elements in soils and plants* (4th ed.). Boca Raton, FL: CRC Press.

Knudson, K. J., Frink, L., Hoffman, B. W., & Price, T. D. (2004). Chemical characterization of Arctic soils: Activity area analysis in contemporary Yup'ik fish camps using ICP-AES. *Journal of Archaeological Sciences*, *31*(4), 443–456.

Kylander, M. E., Ampel, L., Wohlfarth, B., & Veres, D. (2011). High-resolution X-ray fluorescence core scanning analysis of Les Echets (France) sedimentary sequence: New insights from chemical proxies. *Journal of Quaternary Science*, *26*(1), 109–117.

Kühtreiber, T. (2014). The investigation of domesticated space in archaeology- architecture and human beings. In S. M. Kristiansen & K. Giles (Eds.), *Dwellings, identities and homes: European housing culture from the Viking Age to the renaissance* (Vol. 84) Denmark: Jutland Archaeological Society.

Larsson, M. A. (2014). *Vanadium in soils: Chemistry and ecotoxicity*. Unpublished Doctoral Thesis. Swedish University of Agricultural Sciences, Uppsala.

Lefebvre, H. (1991). *The production of space*. Oxford: Blackwell Publishing.

Linderholm, J. (2007). Soil chemical surveying: A path to a deeper understanding of prehistoric sites and societies in Sweden. *Geoarchaeology*, *22*, 417–438.

Løvschal, M. and Holst, M. K. (2014). Repeating boundaries-repertoires of landscape regulations in southern Scandinavia in the Late Bronze Age and Pre-Roman Iron Age. *Danish Journal of Archaeology*, *3*(2), 95–118.

Luzzadder-Beach, S., Beach, T., Terry, R. E., & Doctor, K. Z. (2011). Elemental prospecting and geoarchaeology in Turkey and Mexico. *Catena*, *85*(2), 119–129.

Ma, Y., & Hooda, P. S. (2010). Chromium, nickel and cobalt. In P. S. Hooda (Ed.), *Trace elements in soils* (pp. 461–479). Chichester: John Wiley & Sons.

Macphail, R., Bill, J., Cannell, R., Linderholm, J., & Rødsrud, C. L. (2013). Integrated microstratigraphic investigations of coastal archaeological soils and sediments in Norway: The Gokstad ship burial mound and its environs including the Viking harbour settlement of Heimdaljordet, Vestfold. *Quaternary International*, *315*, 131–146.

Macphail, R., Crowther, J., & Linderholm, J. (2014). *Heimdaljordet, Vestfold, Norway: soil micromorphology, chemistry and magnetic susceptibility*. Unpublished archive report: UCL.

Macphail, R. I., Bill, J., Crowther, J., Haită, C., Linderholm, J., Popovici, D., & Rødsrud, C. L. (2016). European ancient settlements—A guide to their composition and morphology based on soil micromorphology and associated geoarchaeological techniques; introducing the contrasting sites of Chalcolithic Borduşani-Popină, Borcea River, Romania and Viking Age Heimdaljordet, Vestfold, Norway. *Quaternary International*, *460*, 30–47.

Mayer, B., Prietzel, J., & Krouse, H. R. (2001). The influence of sulfur deposition rates on sulfate retention patterns and mechanisms in aerated forest soils. *Applied Geochemistry*, *16*(9–10), 1003–1019.

Mees, F., & Stoops, G. (2010). Sulphidic and sulphuric materials. In G. Stoops (Ed.), *Interpretation of micormorphological of soils and regoliths* (pp. 543–568). Amsterdam: Elsevier.

Middleton, W. D., & Price, D. T. (1996). Identification of activity areas by multi-element characterization of sediments from modern and archaeological house floors using inductively coupled plasma-atomic emission spectroscopy. *Journal of Archaeological Sciences*, *23*, 673–687.

Middleton, W. D. (2004). Identifying chemical activity residues on prehistoric house floors: A methodology and rationale for multi-elemental characterization of a mild acid extract of anthropogenic sediments. *Archaeometry*, 46(1), 47–65.

Middleton, W. D., Barba, L., Pecci, A., Burton, J. H., Ortiz, A., Salvini, L., & Suárez, R. R. (2010). The study of archaeological floors: Methodological proposal for the analysis of anthropogenic residues by spot tests, ICP-OES, and GC-MS. *Journal of Archaeological Method and Theory*, 17(3), 183–208.

Mikołajczyk, Ł., & Schofield, J. E. (2017). A geochemical signal from a Mesolithic Intertidal Archaeological Site: A proof-of-concept study from Clachan Harbor, Scotland. *Geoarchaeology*, 32(3), 400–413.

Milek, K. B., & Roberts, H. M. (2013). Integrated geoarchaeological methods for the determination of site activity areas: A study of a Viking Age house in Reykjavik, Iceland. *Journal of Archaeological Sciences*, 40(4), 1845–1865.

NIBIO. (2018). Kilden. Aas: NIBIO (Norwegian Institute for Bioeconomy Research) Online database. Retrieved from https://kilden.nibio.no/

Oonk, S., Slomp, C., & Huisman, D. (2009). Geochemistry as an aid in archaeological prospection and site interpretation: Current issues and research directions. *Archaeological Prospection*, 16, 35–51.

Oonk, S., Slomp, C. P., Huisman, D. J., & Vriend, S. P. (2009). Effects of site lithology on geochemical signatures of human occupation in archaeological house plans in the Netherlands. *Journal of Archaeological Sciences*, 36(6), 1215–1228.

Ottaway, J. H., & Matthews, M. R. (1988). Trace element analysis of soil samples from a stratified archaeological site. *Environmental Geochemistry and Health*, 10(3), 105–112.

Rødsrud, C. L. (2014). *Markeds/Produksjonplass og Gravfelt*. Gokstad Nedre 48/2, 46/4, Sandefjord, Vestfold. Unpublished archive report, Museum of Cultural History: University of Oslo.

Salisbury, R. B. (2013). Interpolating geochemical patterning of activity zones at Late Neolithic and Early Copper Age settlements in eastern Hungary. *Journal of Archaeological Sciences*, 40(2), 926–934.

Schiffer, M. B. (1976). *Behavioral archeology*. New York, NY: Academic Press.

Schneidhofer, P., Nau, E., Hinterleitner, A., Lugmayr, A., Bill, J., Gansum, T., ... Trinks, I. (2017). Palaeoenvironmental analysis of large-scale, high-resolution GPR and magnetometry data sets: The Viking Age site of Gokstad in Norway. *Archaeological and Anthropological Sciences*, 9(6), 1187–1213.

Skre, D. (2007). Introduction. In D. Skre (Ed.), *Kaupang in Skiringssal* (Vol. 1, pp. 13–24). Aarhus: Aahus University Press.

Solbakken, E., Nyborg, Å., Sperstad, R., Fadnes, K., & Klakegg, O. (2006). Viten fra Skog og Landskap. Jordmonnsatlas for Norge: Beskrivelse av jordsmonn på dyrkamark i Vestfold Ås: Norsk Institutt for Skog og Landskap.

Speakman, R. J., & Shackley, S. M. (2013). Silo science and portable XRF in archaeology: A response to Frahm. *Journal of Archaeological Sciences*, 40(2), 1435–1443.

Stacey, S. P., McLaughlin, M. J., & Hettiarachchi, G. M. (2010). Fertilizer-borne trace element contaminats in soils. In P. S. Hooda (Ed.), *Trace elements in soils* (pp. 134–154). Chichester: John Wiley & Sons.

Sylvester, G. C., Mann, A. W., Rate, A. W., & Wilson, C. A. (2017). Application of high-resolution Mobile Metal Ion (MMI) soil geochemistry to archaeological investigations: An example from a Roman metal working site, Somerset, United Kingdom. *Geoarchaeology*, 32(5), 563–574.

Sørensen, R., Henningsmoen, K. E., Høeg, H., Stabell, B., & Bukholm, K. M. (2007). Geology, soils, vegetation and sea-levels in the Kaupang Area. In D. Skre (Ed.), *Kaupang in Skiringssal* (Vol. 1, pp. 251–272). Aarhus: Aarhus University Press.

Tan, K. H. (1994). *Environmental soil science*. New York, NY: Marcel Dekker Inc.

Tan, K. H. (1998). *Principles of soil chemistry* (3rd ed.). New York, NY: Marcel Dekker, Inc.

Trinks, I., Hinterleitner, A., Neubauer, W., Nau, E., Löcker, K., Wallner, M., ... Seren, S. (2018). Large-area high-resolution ground-penetrating radar measurements for archaeological prospection. *Archaeological Prospection*, 25(3), 171–195.

Tuan, Y.-F. (1977). *Space and place, the perspective of experience*. London: Edward Arnold.

Vyncke, K., Waelkens, M., Degryse, P., & Vassilieva, E. (2011). Identifying domestic functional areas. Chemical analysis of floor sediments at the Classical-Hellenistic settlement at Düzen Tepe (SW Turkey). *Journal of Archaeological Sciences*, 38(9), 2274–2292.

Walkington, H. (2010). Soil science applications in archaeological contexts: A review of key challenges. *Earth Science Reviews*, 103, 122–134.

Wallace, P. F. (2016). *Viking Dublin: The Wood Quay excavations*. Sallins, Co. Kildare: Irish Academic Press

Wells, E. C., Terry, R. E., Parnell, J. J., Hardin, P. J., Jackson, M. W., & Houston, S. D. (2000). Chemical analyses of ancient anthrosols in residential areas at Piedras Negras, Guatemala. *Journal of Archaeological Sciences*, 27(5), 449–462.

White, R. E. (2006). *Principles and practice of soil science: The soil as a natural resource* (4th ed.). Oxford: Blackwell Science Ltd.

Wilson, C. A., Davidson, D. A., & Cresser, M. S. (2007). Evaluating the use of multi-element soil analysis in archaeology: A study of a postmedieval croft (Olligarth) in Shetland. *Atti della Società Toscana*, 112, 69–78.

Wilson, C. A., Davidson, D. A., & Cresser, M. S. (2008). Multi-element soil analysis: An assessment of its potential as an aid to archaeological interpretation. *Journal of Archaeological Sciences*, 35(2), 412–424.

Wilson, C. A., Davidson, D. A., & Cresser, M. S. (2009). An evaluation of the site specificity of soil elemental signatures for identifying and interpreting former functional areas. *Journal of Archaeological Sciences*, 36(10), 2327–2334.

## SUPPORTING INFORMATION

Additional supporting information may be found online in the Supporting Information section.